The Effects of Sputtering and Blistering on the UWCTR First Wall

R.G. Brown

May 1973

UWFDM-60

FUSION TECHNOLOGY INSTITUTE

UNIVERSITY OF WISCONSIN

MADISON WISCONSIN

The Effects of Sputtering and Blistering on the UWCTR First Wall

R.G. Brown

Fusion Technology Institute
University of Wisconsin
1500 Engineering Drive
Madison, WI 53706

http://fti.neep.wisc.edu

May 1973

UWFDM-60

THE EFFECTS OF SPUTTERING AND BLISTERING ON THE UWCTR FIRST WALL

Robert G. Brown

May 1973

FDM 60

University of Wisconsin

INTRODUCTION

The first wall of a thermonuclear reactor is exposed to high fluxes of charged particles, neutrons, neutral atoms, and gamma rays throughout life. Primary and secondary interaction processes will occur which can result in a degradation of mechanical properties and an effective erosion of the first wall. Primary reactions may be defined as those interactions between the incident ion and the target where a momentum transfer occurs, a change in the internal energy state of one or both particles occurs, or a nuclear reaction takes place.[2] As a result of these, secondary processes such as lattice atom displacement, or ionization and x-ray emission may occur. These reactions can cause a variety of phenomena: physical and chemical sputtering, blistering, secondary electron emission, x-ray emission, backscattering of particles and photons, release of absorbed and adsorbed gases, radiation damage, photodecomposition of surface compounds, particle entrapment, and re-emission of trapped particles.[2,7,9] An illustration of the various phenomena can be seen in Figure 1.

Although several of the above processes have been investigated, very little experimental data is available for the extreme environment and the various types of metals that would be found in a fusion reactor. Of these processes, sputtering and blistering appear to be the most significant in influencing the first wall lifetime and as such will be the only phenomena considered here. Sputtering and blistering have two deleterious effects on the CTR system. The first is an

an effective erosion or thinning of the first wall. The atoms removed by these processes can also return to the plasma and in some systems cause power losses that will cool the plasma below the minimum temperature needed to sustain the fusion reaction. The effects of sputtering and blistering on fusion reactors, particularly the UWCTR, will be discussed following a brief review of the theory and experimental results pertaining to these phenomena.

SPUTTERING

Bombarding a metallic target by high energy ions, neutrons, or neutral atoms will displace atoms in the target from their lattice sites. Not all of these displaced atoms remain in the target. They may be sputtered off the front surface of the target and ejected from the back surface. The phenomena whereby atoms are ejected from the lattice only by momentum transfers in the collision process is termed physical sputtering.[1] This is to be distinguished from chemical sputtering. In chemical sputtering, a reactive ion and the target atom form a volatile compound which can leave the target surface.[1] The kinetic energy of the incident particle is less important in chemical sputtering than in physical sputtering. In many irradiation environments, both physical and chemical sputtering contribute to the overall removal rate.[2] This paper will consider only the physical sputtering process.

Several theoretical studies on sputtering have been developed[4-6] and good reviews of the theory presented.[1,32]

Two of the more prominent sputtering models will be discussed briefly.

Hot Spot Model

The "hot spot" or "heated spike" model describes sputtering as an "evaporation" of atoms off the surface. The incident ion heats the local region of the metal in the vicinity of collision. The local temperature becomes so high that atoms leave the surface by an evaporation process. According to Pease,[4] this model is likely to be incorrect for most applications. This is because the sputtering is based on the macroscopic concepts of thermodynamics. Pease states that

if the hot spot has linear dimensions longer than the mean free path of photons and/or electrons, and the hot spot exists for a longer time than the frequency of thermal oscillations of the lattice atoms, then the hot spot model may be applicable.[4]

Kaminsky has summarized the drawbacks of this model.[1] First the hot spot model does not predict the angular distribution of the sputtered particles in either the high or very low energy ranges. The model also does not explain the dependence of sputtering upon the angle of incidence of the bombarding ion. The hot spot model also incorrectly predicts the energy distribution of the sputtered particles. The mean energies of sputtered particles are orders of magnitude higher than thermal energies. Despite these inadequacies in the model, Kaminsky states that it may have some use in conjunction with a collision model.

Collision Models

Collision models treat sputtering by analyzing the individual collisions of the incident ion and its primary knock-on atoms (PKA's) in the lattice. The displaced atoms in the lattice all slow down by undergoing further collisions. As this occurs, they may diffuse and escape. Also, collisions beneath the surface may result in focusing events which transfer momentum along close-packed rows of atoms. If these close-packed rows terminate on the surface, enough energy might be imparted to the atom at the surface so that it is ejected from the surface.

The collisions in the lattice may be treated as falling into one of three groups, depending on the incident particle energy and the distance of closest approach.[1,4] The potential describing the interaction between the projectile and target atom is assumed to be a screened Coulomb potential.[1,4]

$$V(r) = \frac{Z_1 Z_2 e^2}{r} \exp\left[-\frac{r}{a}\right] \qquad (1)$$

where Z_1 and Z_2 are the atomic numbers of the projectile and target atom, respectively.

e is the charge on an electron.
r is the distance between the two nuclei.
a is the electron cloud radius defined by

$$a = \frac{a_o}{(Z_1^{2/3} + Z_2^{2/3})^{1/2}} . \qquad (2)$$

a_o is the Bohr radius.

For incident ions having a high enough energy so that the electron clouds around the nucleus are penetrated, the interaction will be through the Coulomb repulsion of the nuclear charges. This interaction is referred to as Rutherford scattering and occurs for all ions with energy greater than E_B where

$$E_B = 4E_R^2 \; Z_1 \; Z_2 \; (Z_1^{2/3} + Z_2^{2/3})^{1/2} \; \frac{M_1}{M_2} \; \frac{1}{E_d} \qquad (3)$$

where E_R is the Rydberg energy (13.68 eV),
E_d is the displacement energy for the lattice atom,
M_1 and M_2 are the atomic weights of the projectile and target atoms, respectively.

Typical values of E_B for various projectiles of interest in CTR applications are listed in Table I.

For energies less than E_B, electron screening becomes important. The lower limit for the use of a weakly screened Coulomb interaction is given by

$$E_A = 2E_R \; Z_1 \; Z_2 \; (Z_1^{2/3} + Z_2^{2/3})^{1/2} \; \frac{M_1 + M_2}{M_2} \qquad (4)$$

Weakly screened interactions may be assumed to occur for particle energies between E_A and E_B.

The final type of collisions that will be considered are for energies much smaller than E_A where there is very little electron cloud penetration. In this region, the collisions are of the hard sphere type. There is also a lower threshold below which no sputtering will occur. This value varies from 12 to about 30 eV.[2] Attempts have been made to measure a threshold energy for sputtering experimentally, but sputtering yields are so low at these energies that a definite threshold is hard to pinpoint.[1] The value of the sputtering threshold will depend both on the incident ion and the target material. Extrapolation of higher energy sputtering data to zero sputtering yield has yielded values as low as 4 eV (for Ar^+ on a silver target).[1]

It should be mentioned that the energy boundaries just described are approximate. To obtain a better prediction of the interactions, an interaction potential should be used that describes collisions for all distances of closed approach that span the gap from simple Coulomb to hard sphere type collisions. However, no one potential describes the entire range of interactions. Use of various other potential models proposed makes the analysis much more complex.

In predicting the rate at which sputtering will erode a surface, a factor called the sputtering ratio is often computed. The sputtering ratio is simply the number of atoms sputtered off the wall per incident particle striking the wall. Several theories have been proposed to predict[4,5,36] this value and a good summary of these can be found in

references 1 and 32. A brief outline of the model proposed by Pease[4] is presented below.

In calculating the sputtering yields, the displacement cross sections for each of the energy regions mentioned above must be known. These relations are listed below.[4]

$E > E_B$

$$\sigma_d = \frac{4\,\pi a_o^2\; M_1\; Z_1^2\; Z_2^2\; E_R^2}{M_2\; E_d}\;\frac{1}{E}\left(1 - \frac{E_d}{E_{max}}\right) \qquad (5)$$

$E_A < E < E_B$

$$\sigma_d = \pi a^2 \qquad (6)$$

$E < E_A$

$$\sigma_d = \pi R^2 \left(1 - \frac{E_d}{E_{max}}\right) \qquad (7a)$$

or

$$\sigma_d = \pi \left[b \ln\left(\frac{M_2}{M_1 + M_2} \cdot \frac{E}{A}\right)\right]^2 \left(1 - \frac{E_d}{E_{max}}\right) \qquad (7b)$$

where R is the distance of closest approach in hard sphere scattering. The minimum value of R can be found by noting that at the distance of closest approach, the relative energy of the neutron-nucleus system must equal the potential energy. Using a Born-Mayer potential, $V(r) = A \exp(-r/b)$, a value of R was calculated and inserted in equation (7a) to yield the expression (7b). A and b are constants determined by compressibility experiments.

E_{max} is the maximum possible energy transfer to the PKA given by

$$E_{max} = 4\,\frac{M_1\; M_2}{(M_1 + M_2)^2}\; E \qquad (8)$$

Pease[4] next considers the penetration of the ion. A solid having an atom number density n may be treated as a series of layers having a density of $n^{2/3}$ per unit area separated by a distance $n^{-1/3}$ (the interatomic spacing). If the product $\sigma_t n^{2/3}$ is on the order of one or greater than one, then it is assumed that the ion will be stopped or reflected at the surface (σ_t is the total cross section). Since the cross sections are uncertain, the energy at which this occurs is not well defined. Pease[4] thus assumes that this energy is the energy such that

$$(\sigma_t n^{2/3}) \times (\text{number of layers}) = 1 \qquad (9)$$

The number of layers where sputtering is of importance is next computed. Knowing this and the average PKA energy, an estimate can be made of the number of atoms sputtered.

The mean energy $\bar{E}$ of the PKA's is not very large. Goldman and Simon[5] assume that the initial collision between the incident ion and the target atom is a simple Coulomb interaction, and all of the interactions by the PKA with other lattice atoms are hard sphere type. The number of collisions N by the PKA in slowing down to an energy below the surface binding energy E_s is given by[4]

$$2^N = \frac{\bar{E}}{E_s} \qquad (10)$$

When the PKA slows down below E_s, which is on the order of 5 eV, it can not escape the surface of the target. N typically has values between 2 and 10. Pease[4] assumes that the PKA's will diffuse about $N^{1/2}$ interatomic layers into the surface. Including the surface layer, the total average number of atomic layers that contribute to sputtering is given by

$$1 + N^{1/2} = 1 + \left[\frac{\log(\bar{E}/E_s)}{\log 2}\right]^{1/2} \tag{11}$$

The total number of atoms displaced per PKA of energy $\bar{E}$ is given by the Kinchin and Pease[20] model to be

$$\nu(\bar{E}) = \frac{\bar{E}}{2E_d} \tag{12}$$

Assuming half of these migrate toward the surface and that they diffuse about the same distance as the PKA's, the sputtering ratio S, is

$$S = (\sigma_d \bar{E} n^{2/3}) \frac{1}{4E_d} \left\{1 + \left[\frac{\log(\bar{E}/E_s)}{\log 2}\right]^{1/2}\right\} \tag{13}$$

for normal incidence and $2E_d < \bar{E} << E_{max}$. The first group of terms represents the mean energy deposited in each layer due to a primary event. The second factor is one-half the average number of displacements per unit of energy. The last term, as described above, estimates the number of atomic layers contributing to sputtering.

Figure 2 shows the results of applying the above result to the bombardment of silver by several ions of various energies.* The variation of S with energy is quite evident. For $E < E_A$, the sputtering ratio increases sharply above some threshold energy and then levels off. The reason for the rapid rise in S is that the average energy transferred to the PKA increases in direct proportion to the initial particle energy in hard sphere scattering. From equation (13), an increase in $\bar{E}$ raises S. Also, a higher initial energy, $\bar{E}$, results in an increase in the displacement cross section, σ_d (see equation (7b)). Note that the

*The symbols L_A and L_B used in Figure 2 correspond to E_A and E_B in the above equations.

threshold energy for sputtering predicted by the Pease model[4] is an order of magnitude higher than Kaminsky's values[2] presented earlier. In the region around E_A, sputtering yields are maximum and decrease slightly over the range from E_A to E_B. In the Rutherford scattering region ($E > E_B$), S decreases with increasing particle energy. Equation (13) shows that S depends strongly on the displacement cross section σ_d and the average energy transferred to a PKA. Equation (5) shows that σ_d is proportional to 1/E above E_B. Also, the average energy transferred to a PKA in Rutherford Scattering is very small and increases only slightly with large increases in incident particle energy. For these reasons, the sputtering ratio will tend to drop above E_B.

Pease[4] explains that his model is most accurate at the higher energies, $E > E_B$, where the only large uncertainty affecting S is the displacement energy. Application of this model below E_B is uncertain since the cross sections are not well known, and the energy spectrum of the PKA's changes more rapidly with ion energy. Experimental results have also shown that when $E > E_B$ the charge (neutral, single, or doubly charged) of the bombarding particle does not affect the sputtering yield.[7] Table II shows some calculations of sputtering ratios for various ions and metals of interest in CTR's. Calculations were made using the above model and another relation derived by Goldman and Simon.[5]

Self Sputtering

The values of the sputtering ratios in Table II are for the light ions that leak out of plasma and strike the first wall. Much more serious erosion will occur if the projectile atom is heavier. Atoms sputtered off the vacuum wall in a CTR may enter the plasma where they gain energy through collisions with the plasma ions. If these atoms return to the wall, self sputtering can result. Summers et. al.[6] have measured sputtering ratios for Nb^+ ions with energies of 10 to 80 KeV on a niobium target at 50 to 100°C. The results are illustrated in Figure 3. Sputtering coefficients are greater than one atom per Nb^+ ion over this energy range. This is due mainly to the high average energy transfer from a niobium ion colliding with a niobium atom. Most of the self-sputtering collisions that occur in a CTR will be in the hard sphere region ($E < E_A$). In the hard sphere region, the average energy transfer is one-half of the maximum possible energy transfer (E_{max}). From the relation for E_{max} it is easily seen that maximum and average PKA energies are highest when $M_1 = M_2$ i.e. self-sputtering. Summers et. al.[6] have calculated that the flux of 20 KeV Nb^+ ions needed to produce a given level of erosion is only 1/200 the flux of deuterium, tritium and helium ions necessary to cause the same damage.

Neutron Sputtering

As well as ion and neutral atom bombardment, the first wall of a CTR will be subjected to high neutron fluxes as well. Added to the incident 14 MeV neutron flux is an even higher flux of "back streaming"

neutrons that come fron (n,2n) reactions in the blanket and from backscattering.[3] The energies of the back streaming neutrons range from about 0.1 to 6 MeV.[3] As can be seen by the following example, neutron sputtering may be a serious problem in CTR systems.[2,7]

Consider the irradiation of a niobium target by separate beams of 14 MeV neutrons and 14 MeV deuterons. The cross section for elastic scattering of a 14 MeV neutron is on the order of 2 barns.[2,7] A 14 MeV deuteron has a displacement cross section of 4800 barns. The average energy of the neutron produced PKA is approximately 146 KeV. The D^+ produces a PKA with average energy of 364 eV. Kaminsky[2,7] calculated the average number of displacements produced by each of these ions to be: 2800 displaced atoms per PKA of 146 KeV caused by the neutron; and 5.4 displaced atoms per 364 eV PKA produced by the deuteron. Thus, although the cross section is 3 orders of magnitude less for neutron reactions, the number of displacements per PKA is almost 3 orders of magnitude higher for neutrons. Kaminsky[2,7] computed sputtering yields for these two particles and found slightly higher values for the 14 MeV neutrons.

Very little consistent data is present on neutron sputtering. Garber et. al.[27] have presented results of extensive irradiations for 25 elements by a fission reactor flux of $2 \times 10^{12} n/cm^2 sec$ ($E > 1$ MeV). They discovered that there is a periodic dependence of the sputtering yield on the atomic number of the target. Their results are given in Figure 4. Both polycrystalline and monocrystalline targets were used. It was found that sputtering from single crystals

was consistently higher by a factor of 1.5 to 2.5.[27] From their work, it can be seen that if a sputtering ratio is known for a given element, it is possible to estimate the sputtering for any other target.

Effect of Irradiation Parameters on Sputtering

The irradiation environment of the metallic surface will be influential in determining the sputtering yields. The effects of certain variables on sputtering are not completely understood, so only a brief description will be presented. The effect of projectile energy was discussed earlier.

Little effect of target temperature on the sputtering yield has been observed.[1,14] The yields seem to be independent of temperature below about 0.8 T_m (T_m is the absolute melting temperature).[14] Above this temperature, sputtering ratios increase up to the melting point. Raising the target temperature increases the thermal vibrations of the target. This can disrupt the transfer of momentum along rows of atoms in a given direction. This defocusing reduces the sputtering off the surface. An increase in temperature can also have an opposite effect. At high enough temperatures, annealing can occur. This reduces the damage level of the material and would tend to increase sputtering.[32]

Sputtering yields are also affected by the angle of incidence of the projectiles impinging upon the surface. Figure 5 shows that as the angle of incidence increases, the sputtering ratio increases. On the average, when an ion is incident upon a surface it travels the

longest distance from the surface before its first interaction when its path is normal to the target. As the angle of incidence increases, the mean distance from the target surface where the projectile has its first interaction will decrease. When the collision cascades occur closer to the surface, there is a higher number of atoms that are sputtered off the surface. As shown in Figure 5, the dependence of the sputtering ratios on the angle of incidence is more pronounced for the higher ion energies. The maximum in the 27 KeV curve in the figure is caused in part by the increased reflection of the primary ion beam off the surface which occurs at large angles of incidence.[1] In experiments with single crystals, sputtering can be very dependent on the orientation of the incident beam with respect to crystallographic directions. If the beam angle is oriented so collisions occur which result in a higher probability of momentum transfer along a close-packed row toward the surface, sputtering yields will increase.

A series of investigations by Wehner et. al.[37-39] revealed some insight on how sputtering yields vary with target material. Their work showed that the sputtering yields are closely related to the number of d-shell electrons. Those metals with a large number of d-shell electrons generally exhibit higher sputtering yields, while those with few d-shell electrons have lower sputtering ratios. This can be seen if Figures 6 and 7 are compared. Figure 6 shows the number of d-shell electrons in various metals and Figure 7 shows sputtering ratios for these metals for various incident projectiles. The above

phenomena is explained by the fact that metals with fewer d-shell electrons are more "open" electronically. Thus, incident projectiles may penetrate farther below the surface. Sputtering decreases because it is difficult to transfer energy back to the surface. For a metal with a large number of d-shell electrons, the ion ranges are closer to the surface thus decreasing the distance along which energy must be focused to produce sputtering. Thus a slightly higher sputtering yield results. Wehner et. al.[38,39] also found that sputtering yield inversely proportional to the heat of sublimation of the target material. This is shown in Figure 8.

Other factors that may substantially influence the sputtering process are alloying effects and impurities in the metal, and the conditions of the surface. Early studies by Wehner[34] on the irradiation of nickel-based alloys, aluminum alloys, and some steels by 0.1-0.5 KeV Hg^+ ions indicated that the sputtering yields were in much the same as yields of the components themselves. More recent work by Dahlgren and McClanahan[28] has shown that alloying can produce a second phase with a low sputtering yield. Since sputtering is dependent on the ability of a matrix to focus energy along a close-packed direction, alloying could interfere with the process by affecting the ordering of the atoms.

Redeposition of sputtered wall atoms on the surface should also reduce the erosion rate.[8] A surface that is contaminated will also tend to lower the sputtering yield. Such surface contaminants that might be found on the vacuum wall of a CTR are oxide layers, adsorbed residual gases, and bulk contamination that has diffused to the surface during the baking cycle.[14] Increased surface roughness caused by

sputter etching, blistering, uneven redeposition, or an intentional etching treatment will also reduce the sputtering yield.

BLISTERING

Irradiation induced blistering is caused by the formation of gas bubbles near the surface of an irradiated metal. This phenomena has been observed following irradiation of various metals by the noble gas ions of helium and argon.[21,23,24,29] An example of blistering by helium ion irradiation is shown in Figure 9. Blistering has also been observed after irradiation by hydrogen and deuterium ions.[2,15,22,24] Blister formation from these latter two ions would not normally be expected due to their high solubility and diffusivity in metals.[2] During irradiation these gas atoms coalesce into bubbles and migrate to regions of lower surface energy such as grain boundaries, dislocation lines, and the surface of the metal.[2] It may also be possible for gas atoms to fill vacancy clusters produced by displacement spikes or convert small voids into bubbles.

On the surface of the metal, these bubbles may eventually rupture releasing the gas contained in them. The thin layer of metal which once covered the bubbles may flake off the surface thus decreasing the thickness of the metal. Blisters may then form, or may have already begun to form, on the newly exposed surface. Thus, the process repeats itself.

There has been no adequate theoretical treatment of blistering. Some predictions have been made as to the pressure involved in the gas bubbles.[19] With the knowledge of the volume of the blisters, the amount of helium release can then be estimated. Predictions of the

erosion rate as a result of blistering have been made, but these are based on experimental data and not theory. Experimental results on blistering are also few and as yet the effects of such parameters as irradiation temperature, dose, and microstructure are not well defined. Some of the recent results of ion bombardments on niobium will be briefly summarized to indicate the present level of understanding with regard to blistering.

It is expected that the average range of an ion incident on a surface will be greater when the beam is oriented in a channeled direction.* As a result of channeling, the ions are eventually deposited further from the surface. This should result in fewer bubbles being nucleated close to the surface thus reducing the amount of blistering. The effect of crystallographic orientation on blistering has been studied recently by Kaminsky.[17] Irradiation of a (111) niobium surface with 0.5 MeV He^+ ions to a charge density of 1 coulomb/cm^2 (6.25×10^{18} particles per cm^2) at 900°C resulted in blisters having a "crow-foot" shape. This is shown in Figure 10a. The prongs of the crow-foot shaped blisters are oriented along the {110} planes with the [111] pole as a center. Since the maximum interplanar spacing occurs between the {110} planes, helium atoms may accumulate more readily along these planes. Bubbles would tend to form there first as is observed in Figure 10a. It has also been noted that thermal etch pits in the above shapes result when niobium is heated without irradiation.[30] Thus the above phenomena may involve other factors.

*The mean linear range of a 0.5 MeV He^+ ion in niobium is 1.5 μm.[19]

Kaminsky has also irradiated another niobium monocrystal sample in a similar manner with the beam not oriented in a channeled direction.[17] The blister density was found to increase by about two orders of magnitude when compared to the above work. The average blister size decreased and although some three-pronged blisters were observed, the majority were irregular in shape. Figure 10b shows this surface.

The effects of cold working on blistering have also been investigated by Kaminsky.[17] Cold worked samples of niobium were irradiated at 900°C to a dose of 1 coulomb/cm^2 by 0.5 MeV He^+ ions. Relative large (~6 to ~20 μm in diameter) dome-shaped blisters were observed. (See Figure 10c) These were somewhat smaller and more regular in shape than a cold worked sample irradiated to the same dose at room temperature. Room temperature rests showed extremely large blisters (up to 500 μm diameter).[19] Although these blisters represented a small fraction of the total number of blisters, they occupied a large percentage of the irradiated surface. The thickness of dome-shaped surface was estimated to be 1.2 μm which is only slightly less than the mean range of the bombarding ions.

The degree of blistering observed in annealed niobium is less than that observed in cold worked samples after room temperature irradiations to 0.1 coulomb/cm^2.[19] However, when the dose level is increased to 1 coulomb/cm^2 blistering becomes greater in the annealed niobium.[19] The effect of microstructure on blistering is still inknown, however the above work indicates that for low charge densities, cold working promotes blister formation. It seems that the high dislocation density of cold worked niobium provides more sites for bubble nucleation.

As the dose increases, radiation damage reaches a high enough level in the annealed metal to allow bubbles to nucleate more easily.[19] In cold worked niobium at 1 coulomb/cm^2, the initial cold work induced dislocation structure is less significant in influencing bubble nucleation than is the high damage state that has formed due to irradiation.

Blistering of niobium bombarded by 300 KeV D^+ ions has been examined by Donhowe et. al.[15] at temperatures from 250 to 700°C. No blisters were observed after irradiation to ~10^{19} ions/cm^2 at any irradiation temperatures below 450°C. At 550°C and 650°C, a high density of very small blisters was observed. At 700°C, the average blister size was an order of magnitude higher than at 650°C (average diameter was 0.7 microns at 700°C), while the observed density decreased by greater than 100 over the 650°C observation. The results are summarized in Table III. The authors also presented the possibility of a blistering threshold between 450 and 550°C, but stated that more experiments would be needed to confirm this.[15] These results also indicate that vacancy diffusion may be a controlling factor in the blistering phenomena.[30] The range of temperatures predicted for the blistering threshold corresponds to about 0.3 T_m for niobium. Above .3 T_m, vacancies are mobile and can more easily migrate to the bubbles at the surface. Below this temperature, where blisters were not seen the vacancies are relatively immobile.

Bauer and Thomas[35] have recently reported some results of 300 KeV helium bombardment of 316 stainless steel in order to compute the helium re-emission rate and examine blistering. The irradiated samples were exposed to a total fluence of 4×10^{18} helium atoms per cm^2 at temperatures from -170°C to 700°C. Scanning electron micrographs of the surface showed that at 300 and 500°C, flaking of the steel surface had occurred. Below about -50°C, surface deformation is caused by blistering. The boundary between the cooler temperature blistering effects and the higher temperature flaking is uncertain but has been estimated at -50°C. Between 600 and 700°C, blisters reappear.

In the intermediate temperature ranges, 300-500°C, a continuous gas filled region formed beneath the surface (near the end of the range of the helium atoms).[35] When the gas pressure is sufficiently high to overcome the strength of the material, the surface layer flakes off. This flaking seems to be periodic with respect to the helium atom dose.

The reappearance of blisters at 600°C is thought to be due to helium bubble formation. Bauer and Thomas[35] found that the helium re-emission is closely related to the surface deformation, and that both surface effects and gas release are closely related to the irradiation temperature.

SURFACE PHENOMENA AFFECTING UWCTR

As the previous section indicates, the surface phenomena effects that will occur on the first wall of a fusion reactor are numerous and not well understood. There are two major problems that will affect CTR design and operation. First, particles that are sputtered off the wall may re-enter the plasma. These atoms will lose electrons in collisions with the plasma ions. As the electrons collide in the plasma, bremsstrahlung is given off. This results in a loss of power in the plasma. If bremsstrahlung losses are high enough, the plasma could be cooled below the temperature needed for operation. Bremsstrahlung losses increase with the atomic number of the foreign atom entering the plasma.[7] Since first wall materials have high atomic numbers, relative to the values present in the plasma, sputtering may result in power loss problems in some reactor situations.[7] However, in the UWCTR design this is not the case and contaminants may actually have to be added to the plasma to keep it from becoming too hot.[30] With this in mind, radiation losses from the plasma caused by sputtering will not be considered here.

The other major problem is erosion of the first wall. Erosion rate estimates due to physical sputtering have been made for niobium first walls for various systems.[2,7-11] These estimates do not consider neutron sputtering, about which very little is known, not has self sputtering been treated in any detail. The erosion rate from the blistering process is also unknown and estimates can only be made based on the scattered data reported. There has been no effort made to treat sputtering off a stainless steel vacuum wall, which is the UWCTR first wall material.

Sputtering Effects in UWCTR

In predicting the erosion rate due to physical sputtering the following relation may be used.[8]

$$N_s = \sum_{\mu} S_{\mu} \phi_{\mu} A t \tag{14}$$

Where N_s is the number of atoms sputtered from the surface.

S_{μ} is the sputtering yield in atoms per particle for a particular bombarding particle μ.

ϕ_{μ} is the flux of the bombarding particle.

A is the area being irradiated.

t is the irradiation time.

The summation occurs over all types of particles: neutrons, deuterons, tritons, alpha particles, and impurity ions in the plasma (such as sputtered first wall ions being returned to the wall). The accuracy of the sputtering prediction depends on the knowledge of S_{μ} and ϕ_{μ} which are energy dependent. For the environment present in a fusion reactor, these values are not well known.

The number of sputtered atoms can also be represented by the equation

$$N_s = d(t)A\left(\frac{\rho N_o}{A_w}\right) \tag{15}$$

Where d(t) is the wall thickness removed as a function of time.

ρ is the density of the wall.

A_w is the atomic weight of the wall material.

N_o is Avogadro's number.

Rearranging the two previous equations, an expression for the wall thickness eroded as a function of time is

$$d(t) = \sum_{\mu} S_{\mu}\phi_{\mu} \frac{t\, A_w}{N_o \rho} \tag{16}$$

This equation will be utilized to estimate the erosion due to physical sputtering caused by individual ions and the total erosion rate in the UWCTR.

Figure 11 shows the stress in the first wall as a function of thickness of the wall.[31] It indicates the bounds imposed on the selection of the wall thickness. The high thermal stresses limit the maximum thickness to less than 8 mm. Approximately 2 mm will be needed to withstand the hoop stresses present during operation. The vacuum wall thickness for the UWCTR design has been selected as 6 mm.[31] Assuming a total corrosion loss to the lithium coolant of ~2 mm in 20 years (plant lifetime), then the combined effect of all surface phenomena cannot cause a wall erosion of more than 2 mm if the lower design limit is not to be surpassed. If d(t) is allowed to be 2 mm in equation (16), then the time necessary to reach this limit can be calculated for various fluxes of the individual ion.

Deuterium and tritium ion bombardment will be considered first. The average deuteron energy in the UWCTR plasma is 12.4 KeV.[31] The maximum ion flux to the first wall is 10^{15} ions/cm^2sec without a divertor. Of this, 45% is expected to be deuterons, 45% tritium ions, 10% alpha particles in the energy range from 10 to 100 KeV. Assuming a 90% efficient divertor, the fluxes to the first wall are listed below.

TABLE IV

MAXIMUM ION FLUXES TO FIRST WALL IN UWCTR WITH A 90% DIVERTOR

Ion	Energy	Flux
Deuterons	12.4 KeV	$4.5 \times 10^{13} cm^{-2} sec^{-1}$
Tritons	12.4 KeV	$4.5 \times 10^{13} cm^{-2} sec^{-1}$
Alpha Particles	10-100 KeV	$1 \times 10^{13} cm^{-2} sec^{-1}$

Using equation (16), an estimate of the sputtering rate for deuterons and tritons will now be estimated for the UWCTR. There is no sputtering data for stainless steel, however Kaminsky[33] suggests a maximum sputtering yield of 0.01 atoms/ion for deuterium and tritium ions. Using this value, and assuming that the atomic weight of stainless steel is 56 and the density is 8.1 g/cm^3, the sputtering rate for deuterons alone in the UWCTR is 0.0016 mm/year. The sputtering rate for tritium ions is essentially the same. Calculating the number of years needed to reach 2mm erosion limit yields 1230 years for one species and 615 years for both deuterons and tritons at the flux level presently specified. Even if the system had no divertor, the time for the wall to be thinned 2mm by both particle fluxes is 61.5 years, still well above the 20 year plant lifetime. It may be of interest to know the irradiation times required before the 2mm erosion loss limit for the UWCTR first wall is exceeded for various deuteron fluxes. These values can be calculated by solving equation (16) for t and then using d = 0.2 cm. For only one ion specie,

$$t = \frac{d(t)\ N_o \rho}{S_\mu \phi_\mu A_w} \tag{17}$$

Figure 12 shows the time needed to reach the 2mm erosion limit as a function of particle flux for 12.4 KeV deuterium ions on a stainless steel wall. The data plotted is listed in Table V. An identical curve would exist for the effect of 12.4 KeV tritium ions.

TABLE V

TIME REQUIRED FOR VARIOUS FLUXES OF 12.4 KeV D^+ IONS TO ERODE A STAINLESS STEEL FIRST WALL 2mm.

D^+ Flux (ions/cm^2-sec)	Time for 2mm Erosion (years)
1×10^{12}	55,100
1×10^{13}	5510
4.5×10^{13} (UWCTR)	1230
5×10^{13}	1120
1×10^{14}	551
5×10^{14}	112
1×10^{15}	55.1
5×10^{15}	11.2

The same type of calculations will next be considered for alpha particle bombardment on the first wall. The energy spread for alpha particles striking the first wall is much larger than for the deuterium and tritium distribution. Figure 2 shows that the sputtering yield is maximized around the value E_A given by equation (4). For a helium ion incident on silver (Figure 2), $E_A \sim 10$ KeV. Since stainless steel is an alloy, an estimate of E_A is difficult to obtain, however, it will probably be less than that for silver since the major components of stainless steel have atomic numbers less than silver. E_A should be on the order of a few KeV for stainless steel. For purposes of calculations, a value of 10 KeV, the lower limit on the energy range of alpha's striking the wall, was selected for the alpha energy. By assuming this low value, the sputtering effects will be maximized, because as Figure 2 shows, sputtering ratios decrease with increasing

ion energy above E_A.

Again, a lack of experimental data means the sputtering ratio must be estimated. This was accomplished as follows. The stainless steel was assumed to have the sputtering properties of pure iron. This is probably a bad assumption because of the alloying effects discussed earlier. From Figure 7 values of the sputtering yields are given for the irradiation of several metals by 400 eV helium ions. The value for copper is $S_{Cu,.4\ KeV} = 0.21$ and for iron $S_{Fe,.4\ KeV} = 0.11$. If it is assumed that the relative sputtering yield of copper compared to iron is the same at 10 KeV as it is at 0.4 KeV, then provided a value of S for copper at 10 KeV can be found, one can estimate S for iron at 10 KeV. McCracken and Erents[13] have calculated values of the sputtering ratio for helium ions on copper. These are shown in Figure 13. For 10 KeV, $S_{Cu,\ 10\ KeV} \simeq 0.28$ atoms/ion. By the above assumption, the 10 KeV sputtering yield for iron is

$$S_{Fe,\ 10\ KeV} \simeq 0.28\ \frac{0.11}{0.21}$$

$$S_{Fe,\ 10\ KeV} \simeq 0.15\ \text{atoms/ion}$$

Equation (16) is used to estimate the sputtering rate by alpha's in UWCTR. The constants are the same as used earlier only S = 0.15 atoms/ion and $\phi = 10^{13}$ ions/cm^2-sec (from Table IV). A yearly erosion loss of 0.00543 mm is calculated. At this rate, it would take 368 years to erode the wall 2 mm. Clearly, the alpha flux alone presents no problem. However, if there were no divertor, the time to lose 2 mm becomes 36.8 years, and when considered along with other processes, may be of some concern.

It may be of interest to know the exposure times required to reach the 2 mm erosion loss limit for various alpha fluxes. Equation (17) is used for this with the appropriate constants and d = 0.2 cm. The times obtained are listed in Table VI and plotted in Figure 14.

TABLE VI

TIME REQUIRED FOR VARIOUS FLUXES OF 10.0 KeV ALPHA PARTICLES TO ERODE A STAINLESS STEEL FIRST WALL 2mm.

Alpha Flux (ions/cm^2 -sec)	Time for 2mm Erosion (years)
1×10^{12}	3680
5×10^{12}	736
1×10^{13} (UWCTR)	368
5×10^{13}	73.6
1×10^{14}	36.8
5×10^{14}	7.36
1×10^{15}	3.68

Neutron sputtering will be considered next. In calculating the neutron sputtering rate, the energy dependent flux must be known. For calculating neutron sputtering on the first wall, only neutrons with energies $E \gtrsim 0.1$ MeV were considered. This comprises the first 50 groups of the flux spectrum calculated for UWCTR.[30] A listing of these values at the UWCTR first wall is given in Table VII.

In choosing a value for the sputtering ratio, again an estimate must be made. No values have been reported for stainless steel or iron. Experimental values vary by as much as two orders of magnitude for niobium.[3] Kaminsky[3] suggests a value of $S = 5.0 \times 10^{-3}$ atoms per neutron for a primary

neutron flux consisting of 14 MeV neutrons and a secondary neutron flux of 0.1 to 6 MeV neutrons. Although the flux spectra of Kaminsky[3] and the UWCTR are undoubtedly different, this value of S will be assumed for purposes of predicting neutron sputtering in UWCTR. Treating the entire energy range from 0.1 to 14.1 MeV by an effective sputtering yield is clearly a poor method to estimate the erosion rate. However, in view of the uncertainties involved in the value of S, this grouping is not so unreasonable. Assuming Kaminsky's value for the sputtering ratio for niobium and using the results of Garber et. al.[27], a value of the sputtering ratio for iron can be estimated. Using Figure 4, a sputtering yield of 9.1×10^{-3} atoms/neutron was estimated for iron which again will be assumed to behave like stainless steel.

Summing the values in Table VII, the total flux at the first wall is 1.789×10^{14} n/cm^2-sec (E > 0.1 MeV). Using equation (16), the erosion rate for both sides* of the UWCTR vacuum wall is 0.0118 mm/year. The time to erode the wall 2mm would be 170 years. As was done with deuterons and alpha particles, the exposure time required to reach the 2mm erosion limit was calculated for various neutron fluxes. These values are listed in Table VIII and plotted in Figure 15.

*Sputtering occurs off the front and back surfaces of the first wall for neutron irradiation.

TABLE VIII

TIME REQUIRED FOR VARIOUS NEUTRON FLUXES (E > 0.1 MeV)
TO ERODE A STAINLESS STEEL FIRST WALL 2mm

Neutron Flux (n/cm^2-sec)	Time for 2mm Erosion (years)
1×10^{13}	3050
5×10^{13}	610
1×10^{14}	305
1.79×10^{14} (UWCTR)	170
5×10^{14}	61
1×10^{15}	30.5
5×10^{15}	6.1
1×10^{16}	3.05
5×10^{16}	0.61

The value of the sputtering ratio for neutrons incident on niobium that was selected by Kaminsky seems to be somewhat high when compared with the limited data available.[30] A more realistic sputtering value might be estimated from the results of Garber et.al.[40] who predicted a sputtering yield of 3×10^{-3} atoms/neutron for a monocrystalline gold target irradiated by 14 MeV neutrons. Using Figure 4 again, the sputtering yields a gold relative to iron are approximately 9/2. This gives a sputtering yield of 6.67×10^{-4} atoms/neutron for iron. This value is considerably lower than the sputtering ratio of 9.1×10^{-3} used in the above calculations. Based on this lower number, an erosion rate for the UWCTR first wall is 0.00086 mm/yr for neutron sputtering. Two uncertainties should be mentioned with regard to this estimate of

the optimistic neutron sputtering yield for iron. First the sputtering yield for a monocrystal is usually higher than the yield for a polycrystal (See Figure 4). The amount by which it is higher is determined by the orientation of the monocrystal during irradiation. Thus, the use of a monocrystalline gold sputtering ratio as a basis for computing an iron sputtering ratio may yield a slight over-estimate. Also Figure 4, which is used to form a comparison between the sputtering yields for gold and iron, is based on a fission spectrum and not a 14 MeV neutron or a fusion reactor spectrum.

Based on the sputtering rates calculated for neutrons, alphas, deuterons, and tritons, the effect of self-sputtering will now be considered. As mentioned earlier, self sputtering occurs when the atoms removed from the wall enter the plasma, gain energy and are returned to the wall. It should be noted that redeposition of these ions on the wall will reduce the overall erosion rate. This effect will not be considered here.

In calculating the self-sputtering rate, the following assumptions will be made. First, sputtering is assumed to occur uniformly over all first wall surfaces facing the plasma in the reactor. Also, all of the sputtered ions or atoms returning to the wall are distributed uniformly over the vacuum wall area. All atoms sputtered back to the first wall have an energy of 12.4 KeV. Finally, because of the divertor only 10% of the wall atoms sputtered are assumed to return to interact with the wall. The flux of wall atoms (iron) returning to the wall ϕ_{Fe} is approximated by

$$\phi_{Fe} \approx 0.1 \ (S_D \ \phi_D + S_T \ \phi_T + S_\alpha \ \phi_\alpha + S_n \ \phi_n) \qquad (18)$$

Where S_D, S_T, S_α, and S_n are the sputtering yields in atoms/particle for deuterons, tritium ions, alpha particles and neutrons, respectively.

ϕ_D, ϕ_T, ϕ_α, and ϕ_n are the fluxes of deuterons, tritium ions, alpha particles and neutrons, respectively, incident on the first wall.

Substituting the values in equation (18).

$$\phi_{Fe} \approx 0.1 \ [0.01 \text{ atoms/ion } (4.5 \times 10^{13} \text{ ions/cm}^2\text{-sec})$$
$$+ 0.01 \text{ atoms/ion } (4.5 \times 10^{13} \text{ ions/cm}^2\text{-sec})$$
$$+ 0.15 \text{ atoms/ion } (10^{13} \text{ ions/cm}^2\text{-sec})$$
$$+ 0.0091 \text{ atoms/neutron } (1.79 \times 10^{14} \text{ n/cm}^2\text{-sec})]$$

$\phi_{Fe} \approx 3.70 \times 10^{11}$ ions/cm^2-sec returned to the wall.

A self-sputtering coefficient for iron must now be chosen. Based on data presented by Kaminsky,[1] 45 KeV Fe^+ ions incident on iron have a sputtering yield of 3 atoms/ion, see Figure 16. Although no data is presented for the change in the self-sputtering coefficient with energy for iron, there is a curve presented for copper (see Figure 17). Based on this curve, a self-sputtering coefficient of 2.5 is chosen for iron at 12.4 KeV. Using this and the above flux in equation (16), an erosion rate of 0.00335 mm/yr is calculated due to self-sputtering for UWCTR. It should be noted that these values were based on the higher neutron sputtering rates. If the more optimistic (lower) sputtering rate is used, the self-sputtering rate is reduced to 0.00228 mm/year.

One factor that has not been considered in determining the self-sputtering losses is a possible autocatalytic effect. This effect may be described as follows. When the iron ions sputtered off the wall return to the wall from the plasma, they may sputter even more wall atoms from the surface since their sputtering ratio's are greater than 1.0. Some of these newly sputtered atoms will eventually return to the vacuum wall after colliding in the plasma. These will in turn result in more atoms leaving the wall. The cycle will continue and, provided losses to the divertor are not too great, sputtering could increase without bound. However, the system will be "flushed out" at various intervals and a new charge of fuel inserted. This refueling process should remove the sputtered wall atoms from the system. Because the "burn time" for UWCTR is unknown, it is impossible to estimate what effect, if any, the autocatalytic self-sputtering process may have on the system. With this latter uncertainty in mind, the self-sputtering erosion rates were calculated assuming that the autocatalytic effect is negligible.

To estimate the total effect of all the physical sputtering processes, the individual erosion rates are next summed. This is performed in the following Table.

TABLE IX

EROSION RATES FOR PHYSICAL SPUTTERING AT UWCTR FIRST WALL

Particle	Energy	Flux	Erosion Rate
D^+	12.4 KeV	4.5×10^{13} ions/cm^2-sec	0.0016 mm/yr.
T^+	12.4 KeV	4.5×10^{13} ions/cm^2-sec	0.0016 mm/yr.
α	10-100 KeV	1×10^{13} ions/cm^2-sec	0.0054 mm/yr.
n	0.1-14.92 MeV	1.79×10^{14} n/cm^2-sec	0.0118 mm/yr.
Fe^+	12.4 KeV	3.7×10^{11} ions/cm^2-sec	0.0034 mm/yr.
		Total erosion rate equals	0.0238 mm/yr

After 20 years, the wall would be thinned by 0.476 mm. This is well below the 2mm allowable limit. This rate is calculated assuming the high neutron sputtering values occur. The more optimistic ratios result in an erosion rate of 0.0117 mm/year. This gives a 20 year wall thickness loss of 0.234 mm.

It should be mentioned that these erosion rates assume a 90% efficient divertor. Without the divertor, ion flux values increase by a factor of 10, thus raising the sputtering rates. The neutron sputtering rates are not effected. With no divertor present, the total wall thickness lost in 20 years is 2.64 mm for the high neutron sputtering calculations, and 2.40 mm for the optimistic neutron sputtering rates. Clearly a divertor is necessary as both of these values exceed the design limit.

The present UWCTR operates at a neutron wall loading of 0.53 MW/m^2. If for some reason, the power level of the reactor is increased, it is desirable that the effects of sputtering be known. Figures 18 and 19

show the effect of increasing the power on the time required to erode the first wall 2mm. Figure 18 shows the individual effects of all particles considered, plus the total time needed to erode the wall 2mm for various wall loadings. Figure 19 illustrates only the total effect and shows the UWCTR lifetime. These sputtering losses are computed on the basis of the lower, more optimistic neutron sputtering rates. Figure 19 indicates that if UWCTR operated at 4.5 MW/m^2 for 20 years, the first wall would be eroded 2mm. Both these figures assume a 90% efficient divertor. If no divertor were used, these times would be decreased by a factor of nearly 10. In this case, a wall loading of only ~ 0.45 MW/m^2 would result in a 2mm erosion in 20 years.

Blistering Effects in UWCTR

Based on the data of Bauer and Thomas[35] reported earlier, some estimates can be made of the erosion rate that will occur in a 316 stainless steel wall as a result of blistering. Bauer and Thomas[35] find that at 500°C, four layers of the stainless steel surface have been removed by a fluence of 4×10^{18} helium atoms/cm^2, for 300 KeV helium atoms. This corresponds to about one layer removed per 10^{18} helium atoms/cm^2. Knowing the range of 300 KeV helium atoms in steel, the thickness of the removed layer can be estimated. Once this is known, an erosion rate may be estimated. These calculations have been made for UWCTR and are outlined below.[30]

For UWCTR, the helium ion flux is 10^{13} ions/cm^2-sec having energies from 10 to 100 KeV.[31] Since 100 KeV ions have the largest range, they will remove the thickest surface layers and cause the greatest damage. Hence, for purposes of estimating the blistering rate, it will be

assumed that all of the helium ions in UWCTR are 100 KeV. Range data for alpha particles in stainless steel was not readily available, so nickel was used. Nickel has a mass and atomic number close to that of iron (the major constituent of stainless steel), and is itself a major alloying element in 316, so this choice is probably representative. The range of 100 KeV helium ions in nickel is 0.406 mg/cm^2.[41] This is equivalent to a 0.46 μm penetration. Assuming a removal rate of one layer per 10^{18} helium atoms/cm^2, an erosion rate of 4.6×10^{-19} μm per helium atom/cm^2 is predicted. For UWCTR the removal rate R is

$$R = 4.6 \times 10^{-19} \frac{\mu m}{He/cm^2} \cdot 1 \times 10^{13} \frac{He}{cm^2 sec} \cdot 3.15 \times 10^{7} \frac{sec}{yr}$$

$$R = \frac{145\ \mu m}{yr} \quad \text{or} \quad \frac{0.145\ mm}{yr}$$

At the end-of-life (20 years), the wall would be thinned by 2.9 mm by blistering alone.

Thus, it may be that blistering will result in a more serious erosion than sputtering. The uncertainties in these estimates should be mentioned. First of all, they are based on just several data points. The worst conditions possible were chosen for estimating the UWCTR's blistering rate: the highest helium ion energy and the highest wall temperature (500°C). Bauer and Thomas[35] found that the erosion rate at 300°C was slightly less. Use of a lower helium ion energy than 100 KeV will also reduce the erosion since the range will be less. However, only helium blistering was considered. As mentioned earlier, deuterium can cause blistering. The combined effect of helium, deuterium, and tritium ion irradiations on the erosion rate is unknown.

CONCLUSION

The results presented in the previous section indicate that sputtering in the UWCTR design will result in a significant erosion rate, but not high enough to limit the plant lifetime. The effect of blistering is uncertain, but preliminary indications are that it may place more severe restrictions on wall design than sputtering.

These results are quantitatively very approximate due to the lack of knowledge about these phenomena. Some of the uncertainties involved will be reviewed briefly. First of all, the sputtering values reported thus far have been for targets in which the damage levels are not excessive. After several years of operation, the first wall of UWCTR will have a very high concentration of voids and dislocation loops. The effect of sputtering or blistering under such conditions is unknown. A decrease in sputtering might be expected since the damaged state of the matrix should decrease the ability of the steel to focus energy along close packed rows of atoms. As mentioned earlier, the alloying involved in stainless steel could also reduce the sputtering ratios relative to those computed for pure iron by disrupting the focusing sequence.

The surface of the UWCTR is not likely to resemble the relatively "clean" surfaces used in most irradiation experiments. Even before reactor startup, oxide layers and adsorbed gases may be present. After operation, blistering and sputtering will result in an even more complex surface to analyze. The effects of a blistered surface on sputtering yields, and the influence of sputtering on surface bubble formation are unknown.

The first wall of UWCTR will also have temperatures ranging from 300°C to 500°C during steady state operation. This range of temperatures may not affect the sputtering yields directly, since as stated earlier sputtering is not highly temperature dependent. However, the damage state of the matrix, such as void and loop sizes and concentrations, will vary significantly with temperature. Thus indirectly, temperature may affect sputtering. Blistering may show some temperature dependence,[15,35] but the extent of this is unknown.

Another effect that was not considered was the effect of sputtered wall atoms being deposited on the first wall. This will probably reduce the overall erosion rate, and may influence both blistering and sputtering as the wall exposure increases.

Although physical sputtering and blistering will likely be the major phenomena contributing to wall erosion, the many other surface interactions should be investigated to determine their effects on the operation of CTR system. Kaminsky[2] feels that particle emission and flaking caused by bombardment of energetic gamma rays may be a serious problem in fusion reactors and more information is urgently needed.

Specifically with regard to predicting sputtering and blistering rates in UWCTR, irradiation data for 316 stainless steel is needed for all types of fusion reactor particles. This would eliminate a good deal of the uncertainty involved in predicting erosion rates based on sputtering data from other metals. The effect of a complex alloy like stainless steel on sputtering could then be observed. As was mentioned earlier, more data is needed on neutron sputtering to resolve

the great differences (orders of magnitude) in neutron sputtering yields. A better theoretical understanding of blistering is desired, as well as the need for more data. Furthermore, in order to be of use in fusion reactor design, these irradiations should be performed in environments similar to those expected in the reactor. It is most important that the energy of the particle fluxes should simulate as best as possible the conditions existing in the reactor. When results such as these are available, a large part of the uncertainty will be eliminated from the prediction of CTR vacuum wall erosion rates.

REFERENCES

1. M. Kaminsky, Atomic and Ionic Impact Phenomena on Metal Surfaces, (Academic Press, New York), 1965.

2. M. Kaminsky, "Surface Phenomena Leading to Plasma Contamination and Vacuum Wall Erosion in Fusion Reactors and Devices," Proceedings of the Internation Working Sessions on Fusion Reactor Technology, Oak Ridge, Tenn., CONF-710624, p. 86, (June 28-July 2, 1971).

3. M. Kaminsky, "Surface Effects in Thermonuclear Devices and Reactors," presented at the Seventh Symposium on Fusion Technology, Grenoble, France (Oct. 24-27, 1972).

4. R. S. Pease, "Phenomena at Plasma-Solid Boundaries," Rendiconti S.I.F., Corso 13 : 158, (September 1959).

5. D. T. Goldman and A. Simon, "Theory of Sputtering by High-Speed Ions," Phys. Rev. 111 : 383, (July 15, 1958).

6. A. J. Summers, N. J. Freeman, and N. R. Daly, "Sputtering Coefficients of Niobium," Proceedings of the Nuclear Fusion Reactors Conference, BNES, Culham, p. 347 (September 1969).

7. M. Kaminsky, "Plasma Contamination and Wall Erosion in Thermonuclear Reactors," IEEE Trans. NS18, (1971).

8. N. Laegreid and S. D. Dahlgren, "CTR First Wall Sputtering and Wall Life Estimates," (1972), to be published.

9. M. Kaminsky, "Surface Effects," Fusion Reactor First Wall Materials, (ed. L. C. Ianniello), WASH-1206, (Jan. 17-28, 1972).

10. N. Laegreid and S. D. Dahlgren, "Wall Sputtering and Wall Life Criteria," Fusion Reactor First Wall Materials, (ed. L. C. Ianniello), WASH-1206, (Jan. 27-28, 1972).

11. E. E. Donaldson, et. al. "Problem Areas: Surface Phenomena," Fusion Reactor First Wall Materials, (ed. L. C. Ianniello), WASH-1206, (Jan. 27-28, 1972).

12. H. H. Andersen, "The Sputtering Efficiency of Polycrystalline Solids," Rad. Effects 3: 51, (1970).

13. G. M. McCracken and S. K. Erents, "Ion Burial in the Divertor of a Fusion Reactor," Proceedings of the Nuclear Fusion Reactors Conference, BNES, Culham, p. 353, (September 1969).

14. R. Behrisch, "Sputtering in Fusion Reactors," (June 1971), to be published.

15. J. M. Donhowe, et. al., "Radiation Blistering in Niobium," Trans. Am. Nucl. Soc. 15: 36, (June 18-22, 1972).

16. J. Donhowe and G. L. Kulcinski, "Radiation Blistering," Fusion Reactor First Wall Materials, (ed. L. C. Ianniello), WASH-1206, (Jan. 27-28, 1972).

17. M. Kaminsky and S. K. Das, "Effect of Channeling and Irradiation Temperature on the Morphology of Blisters in Niobium," Appl. Phys. Lett. 21: 443, (Nov., 1972).

18. M. Kaminsky and S. K. Das, "Blistering of Polycrystalline and Monocrystalline Niobium," to be published in Rad. Effects.

19. S. K. Das and M. Kaminsky, "Radiation Blistering of Polycrystalline Niobium by Helium-Ion Implantation," to be published in J. App. Phys.

20. G. H. Kinchin and R. S. Pease, "The Displacement of Atoms in Solids by Radiation," Rep. Progr. Phys. 18: 1, (1955).

21. W. Primak, "Radiation-Induced Stress Relaxation in Quartz and Vitreous Silica," J. App. Phys. 35: 1342, (1964).

22. M. Kaminsky, "Mass Spectrometric Studies of the Species of Particles Leaving a Monocrystalline Target in a Charged or Uncharged State Under High Energy Ion Bombardment," Adv. Mass Spectrometry 3: 69, (1964).

23. R. S. Nelson, "The Sputtering of Metals with Noble Gas Ions: an Experiment to Determine the Fate of the Injected Gas and its Influence on the Sputtering Process," Phil. Mag. 9: 343, (1964).

24. M. Kaminsky, "Radiation Blistering in Niobium," Bull. Am. Phys. Soc. 17: 678, (May 1972).

25. M. Kaminsky, "High Energy Ion-Impact Phenomena," J. Vac. Sci. Technol. 8: 14, (1971).

26. M. Kaminsky, "Sputtering Experiments in the Rutherford Collision Region," Phys. Rev. 126: 1267, (May 15, 1962).

27. R. I. Garber, et. al. "Radiation Sputtering and Damage of Certain Metals in the Radiation Field of a Nuclear Reactor. Part I. Sputtering by Fast Neutrons," Atomnaya Energiya 28: 400, (May 1970).

28. S. D. Dahlgren and E. D. McClanahan, "Reduced Sputtering Yields for Two-Phase Ag-Ni and Ag-Co Targets," J. App. Phys. 43: 1514 (April 1972).

29. R. Barnes and D. Mazey, "The Migration and Coolescence of Inert Gas Bubbles in Metals," Proc. Roy. Soc. 275: 47, (1963).

30. G. Kulcinski, personal communication.

31. M. A. Abdou, et. al. "Preliminary Conceptual Design of a Tokamak Reactor," FDM-36, (November 1972), to be published in proceedings of Texas Symposium on the Technology of Controlled Thermonuclear Fusion Experiments and the Engineering Aspects of Fusion Reactors.

32. G. Carter and J. Colligon, Ion Bombardment of Solids (American Elsevier Publishing Co., New York), 1968.

33. M. Kaminisky, personal communication.

34. G. K. Wehner, "Low Energy Sputtering Yields in Hg," Phys. Rev. 112: 1120, (Nov. 15, 1958).

35. W. Bauer and G. J. Thomas, "Helium Re-emission and Surface Deformation in 316 Stainless Steel Suring -170°C to 700°C Implantations," to be published in J. Nucl. Mat.

36. F. Keywell, "Measurements and Collision-Radiation Damage Theory of High-Vacuum Sputtering," Phys. Rev. 97: 1611, (March 15, 1955).

37. G. K. Wehner, "Sputtering Yields for Normally Incident Hg^+ -Ion Bombardment at Low Ion Energy," Phys. Rev. 108: 35, (October 1, 1957).

38. N. Laegreid and G. K. Wehner, "Sputtering Yields of Metals for Ar^+ and Ne^+ Ions with Energies from 50 to 600 eV," J. Appl. Phys., 32: 365, (March 1961).

39. D. Rosenburg and G. K. Wehner, "Sputtering Yields for Low Energy He^+-, Kr^+-, and Xe^+- Ion Bombardment," J. Appl. Phys., 33: 1842, (May 1962).

40. R. Garber et. al., "Radiation Sputtering of a Single Crystal of Gold by Fast Neutrons," JETP Lett. 7: 296 (1968).

41. L. C. Northcliff and R. F. Schilling, "Range and Stopping-Power Tables for Heavy Ions," Nuclear Data Tables 7: 233, (January, 1970).

Table 1

Values of the limiting energies E_A between the hard-sphere collision region and the weakly-screened Coulomb collision region and E_B between the latter and the Rutherford collision region. The projectiles and wall materials shown are some of those of interest for fusion reactors. All energies are in keV.

Projectile	Vanadium		Niobium		Molybdenum	
	E_A	E_B	E_A	E_B	E_A	E_B
H^+	1.9	2.8	4.1	7.0	4.2	7.2
D^+	2.0	5.7	4.1	14.0	4.3	14.5
He^+	4.2	48.3	8.6	117.2	8.9	120.8

M. Kaminsky, "Surface Phenomena Leading to Plasma Contamination and Vacuum Wall Erosion in Fusion Reactors and Devices," Proceedings of the International Working Sessions on Fusion Reactor Technology, Oak Ridge, Tenn., CONF-710624, p. 86, (June 28-July 2, 1971).

TABLE II

Sputtering yields S (atoms/ion) for wall materials and projectiles of interest in fusion reactors. The values calculated according to the theories of Pease (P) and of Goldman and Simon (G) are compared with the experimental values (Exp).

Wall		H^+ Projectile energy E (keV)						D^+ Projectile energy E (keV)					
		10	20	50	100	200	500	10	20	50	100	200	500
V	P	0.0097	0.0061	0.0031	0.0018	0.0010	0.0005	0.0240	0.0150	0.0072	0.0041	0.0023	0.0011
	G	0.0030	0.0018	0.0008	0.0005	0.0003	0.0001	0.0069	0.0040	0.0019	0.0011	0.0006	0.0027
Nb	P	0.0081	0.0056	0.0031	0.0018	0.0011	0.0005	0.022	0.014	0.0073	0.0043	0.0024	0.0011
	G	0.0027	0.0016	0.0008	0.0005	0.0003	0.0001	0.0065	0.0038	0.0018	0.0010	0.0006	0.0003
	Exp							0.0059[c]	0.0040[d]				
									0.0042[e]				
Mo	P	0.0086	0.0060	0.0033	0.0020	0.0012	0.00055	0.0240	0.0150	0.0079	0.0046	0.0026	0.0012
	G	0.0029	0.0018	0.0009	0.0005	0.0003	0.0001	0.0070	0.0042	0.0020	0.0011	0.0006	0.0003
Cu	P	0.0160	0.0100	0.0053	0.0031	0.0018	0.0008	0.041	0.025	0.012	0.0070	0.0039	0.0018
	G	0.0036	0.0021	0.0010	0.0006	0.0003	0.0002	0.0085	0.0049	0.0023	0.0013	0.0007	0.0003
	Exp	0.022[a]				0.0013[b]	0.0010[b]				0.0028[f]	0.0020[f]	0.0011[f]

Wall		He^+ Projectile energy E (keV)					
		10	20	100	500	1000	3500
V	P	0.2300	0.1350	0.036	0.0092	0.0050	0.0017
	G	0.0630	0.0360	0.0093	0.0023	0.0012	0.0004
Nb	P	0.2250	0.1370	0.0390	0.0100	0.0055	0.0018
	G	0.0610	0.0350	0.0093	0.0023	0.0013	0.0004
	Exp		0.051[e]				
Mo	P	0.2410	0.1470	0.0042	0.011	0.0060	0.0020
	G	0.0660	0.0380	0.010	0.0026	0.0014	0.0005
Cu	P	0.3910	0.2300	0.0620	0.0160	0.0085	0.0028
	G	0.078	0.0440	0.0110	0.0028	0.0015	0.0005

[a]Ref. 37. Value measured for 8-keV H^+ on Au.
[b]Ref. 18. Value measured for monocrystalline Cu(111) target, theories not applicable.
[c]Ref. 7. Value measured for 12.2-keV D^+.
[d]Ref. 7. Value measured for 18.8-keV D^+.
[e]Ref. 8. The Nb target temperature was 1100°C.
[f]Ref. 16. Values measured for monocrystalline Cu (100) target, theories
p. 236. not applicable.

M. Kaminsky, "Surface Phenomena Leading to Plasma Contamination and Vacuum Wall Erosion in Fusion Reactors and Devices," Proceedings of the International Working Sessions on Fusion Reactor Technology, Oak Ridge, Tenn., CONF-710624, p. 86, (June 28-July 2, 1971).

TABLE III

RADIATION BLISTERING IN NIOBIUM

	DENSITY	DIAMETER	CONTRAST
700 °C	4×10^6 cm^{-2}	0·7 μ	EXCELLENT
650 °C	1×10^9	0·06	EXCELLENT
550 °C	6×10^8	0·08	POOR
450 °C	NO VISIBLE BLISTERS IN S.E.M.		
350 °C	NO VISIBLE BLISTERS IN S.E.M.		
250 °C	NO VISIBLE BLISTERS IN S·E·M·		

J. M. Donhowe, et. al., "Radiation Blistering in Niobium," Trans. Am. Nucl. Soc. 15: 36, (June 18-22, 1972).

TABLE VII

NEUTRON FLUX AT UWCTR FIRST WALL (0.53 MW/m^2)
FOR ENERGIES GREATER THAN 0.1 MeV

Group Number	Lower Energy of Group (MeV)	Flux (n/cm^2-sec x 10^{13})
1	13.50	5.65
2	12.21	0.341
3	11.05	0.185
4	10.00	0.228
5	9.048	0.191
6	8.187	0.150
7	7.408	0.122
8	6.703	0.107
9	6.065	0.096
10	5.488	0.094
11	4.966	0.091
12	4.493	0.092
13	4.066	0.095
14	3.679	0.104
15	3.329	0.114
16	3.012	0.126
17	2.725	0.146
18	2.466	0.176
19	2.231	0.198
20	2.019	0.202
21	1.827	0.225
22	1.653	0.248
23	1.496	0.259
24	1.353	0.271
25	1.225	0.273

TABLE VII (continued)

Group Number	Lower Energy of Group (MeV)	Flux (n/cm^2-sec x 10^{13})
26	1.108	0.295
27	1.003	0.289
28	0.9072	0.307
29	0.8208	0.309
30	0.7427	0.308
31	0.6721	0.360
32	0.6081	0.372
33	0.5502	0.359
34	0.4979	0.360
35	0.4505	0.368
36	0.4076	0.317
37	0.3688	0.360
38	0.3337	0.321
39	0.3020	0.227
40	0.2752	0.183
41	0.2472	0.089
42	0.2237	0.115
43	0.2024	0.213
44	0.1832	0.289
45	0.1657	0.377
46	0.1500	0.430
47	0.1357	0.374
48	0.1228	0.411
49	0.1111	0.375
50	0.08652	0.748

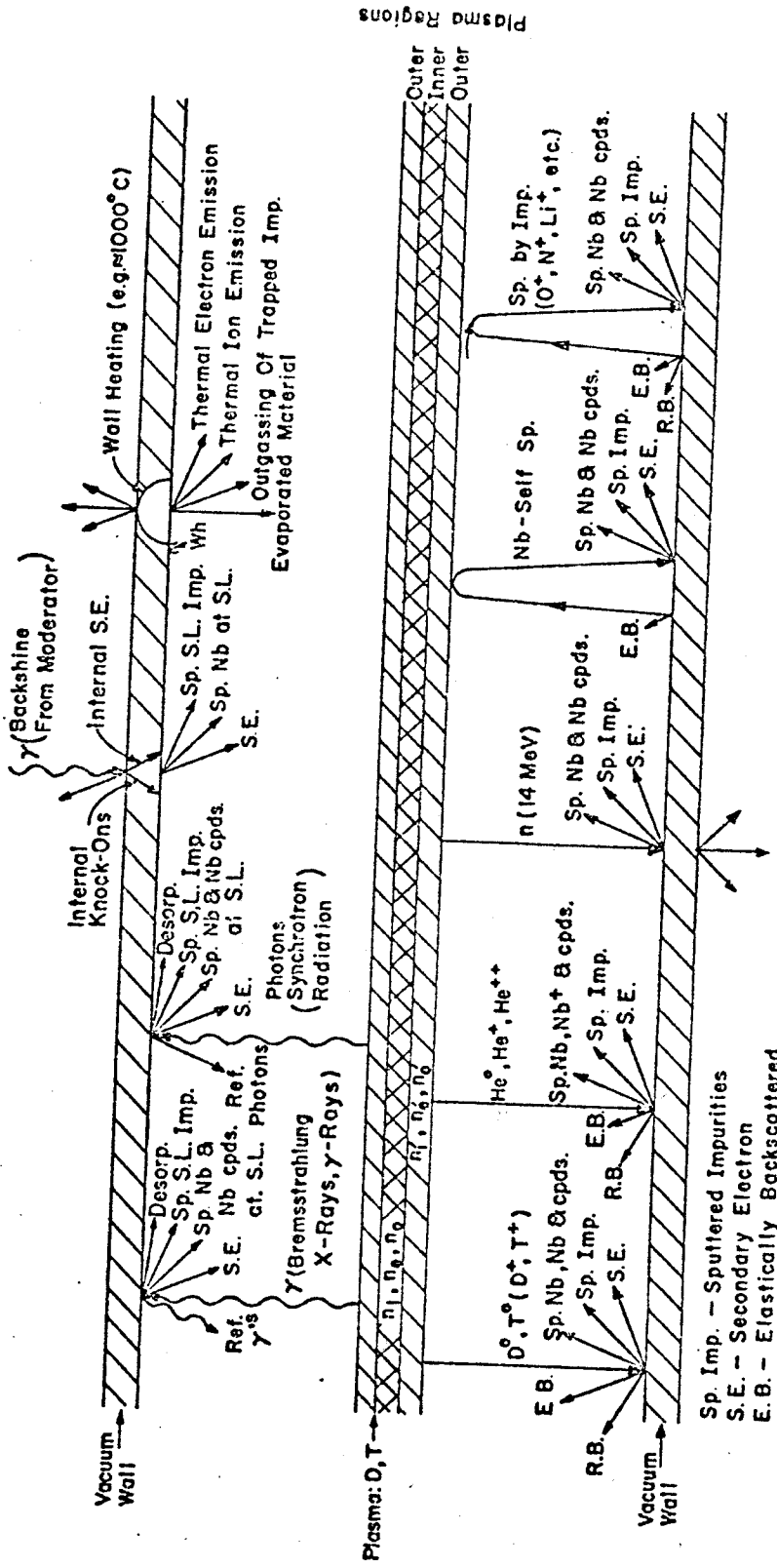

Fig. 1. Secondary phenomena which may occur at the heated walls of a plasma container under the impact of energetic particles and photons.

M. Kaminsky, "Surface Phenomena Leading to Plasma Contamination and Vacuum Wall Erosion in Fusion Reactors and Devices," Proceedings of the International Working Sessions on Fusion Reactor Technology, Oak Ridge, Tenn., CONF-710624, p. 86, (June 28-July 2, 1971).

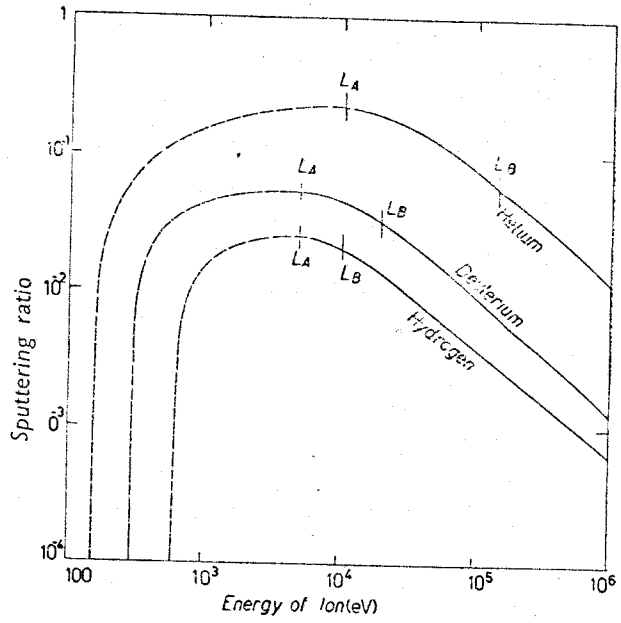

– Calculated sputtering ratio of various ions on silver, as a function of energy. The energy limits for weak screening and hard sphere collision are L_B and L_A respectively. The dashed portion of the curves indicate regions of decreased reliability.

Figure 2

R. S. Pease, "Phenomena at Plasma-Solid Boundaries," Rendiconti S.I.F., Corso 13: 158, (September 1959).

Figure 3

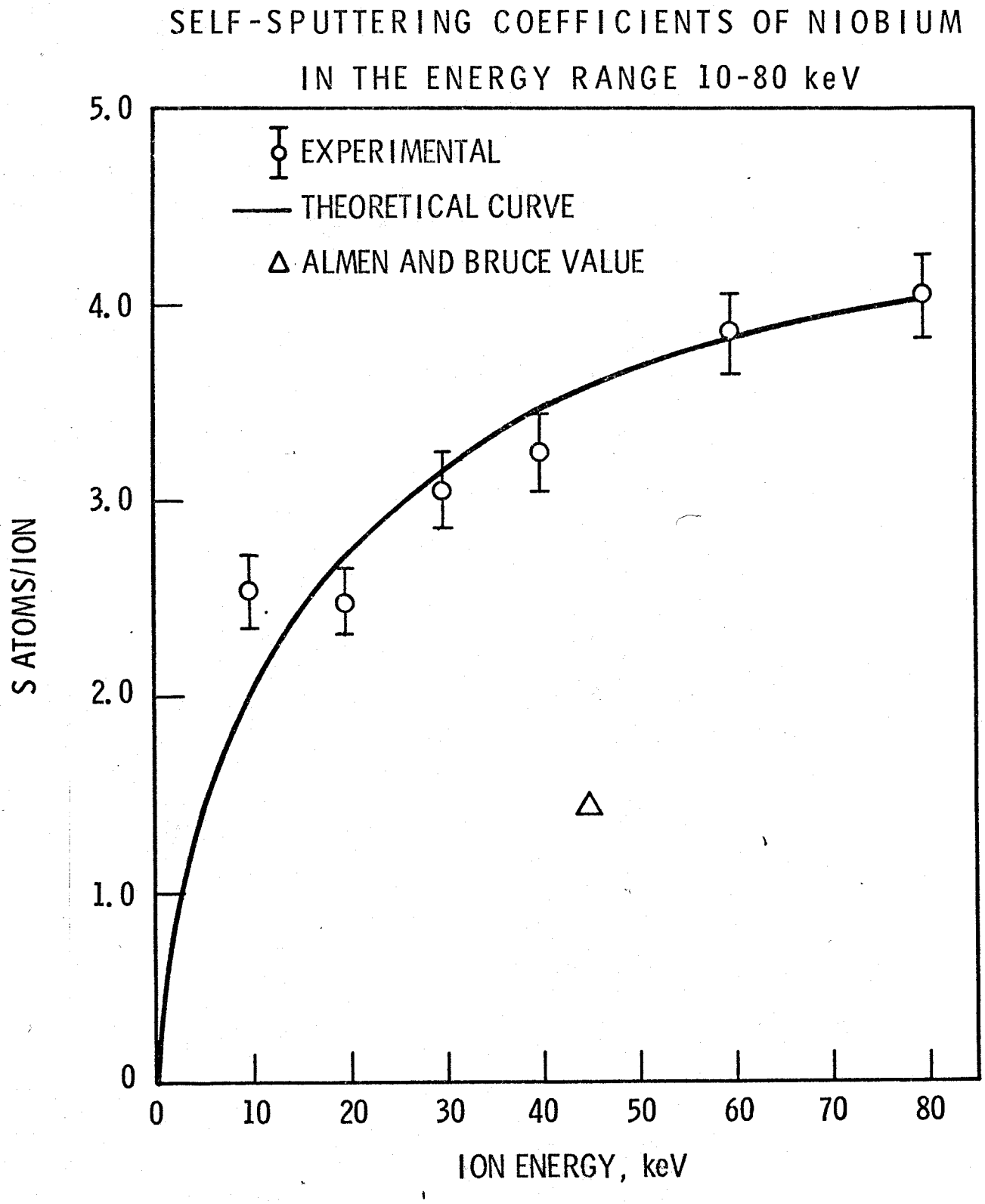

A. J. Summers, N. J. Freeman, and N. R. Daly, "Sputtering Coefficients of Niobium," Proceedings of the Nuclear Fusion Reactors Conference, BNES, Culham, p. 347 (September 1969).

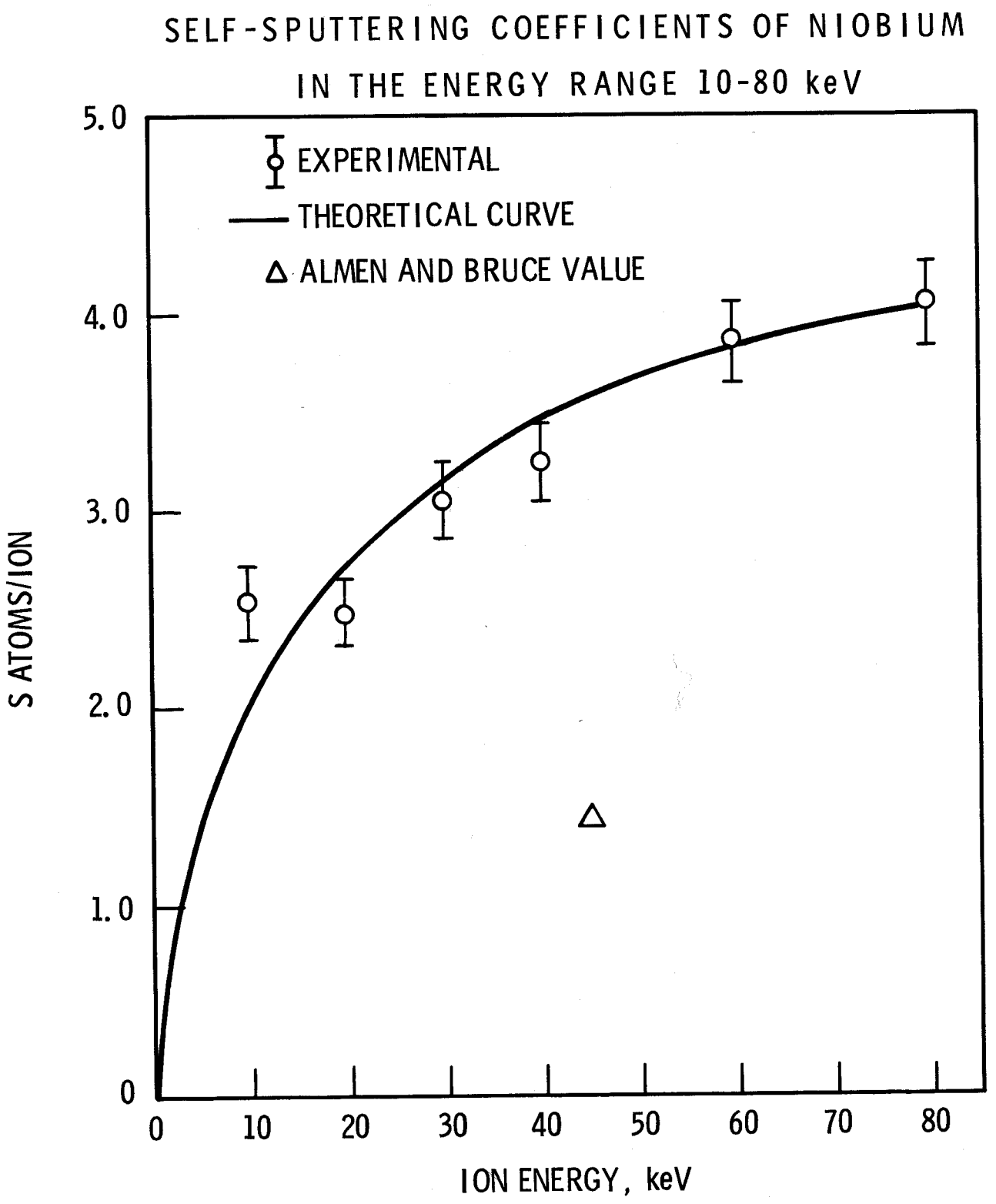
SELF-SPUTTERING COEFFICIENTS OF NIOBIUM
IN THE ENERGY RANGE 10-80 keV
EXPERIMENTAL
THEORETICAL CURVE
ALMEN AND BRUCE VALUE
S ATOMS/ION
5.0
4.0
3.0
2.0
1.0
0
0
10
20
30
40
50
60
70
80
ION ENERGY, keV

Figure 4

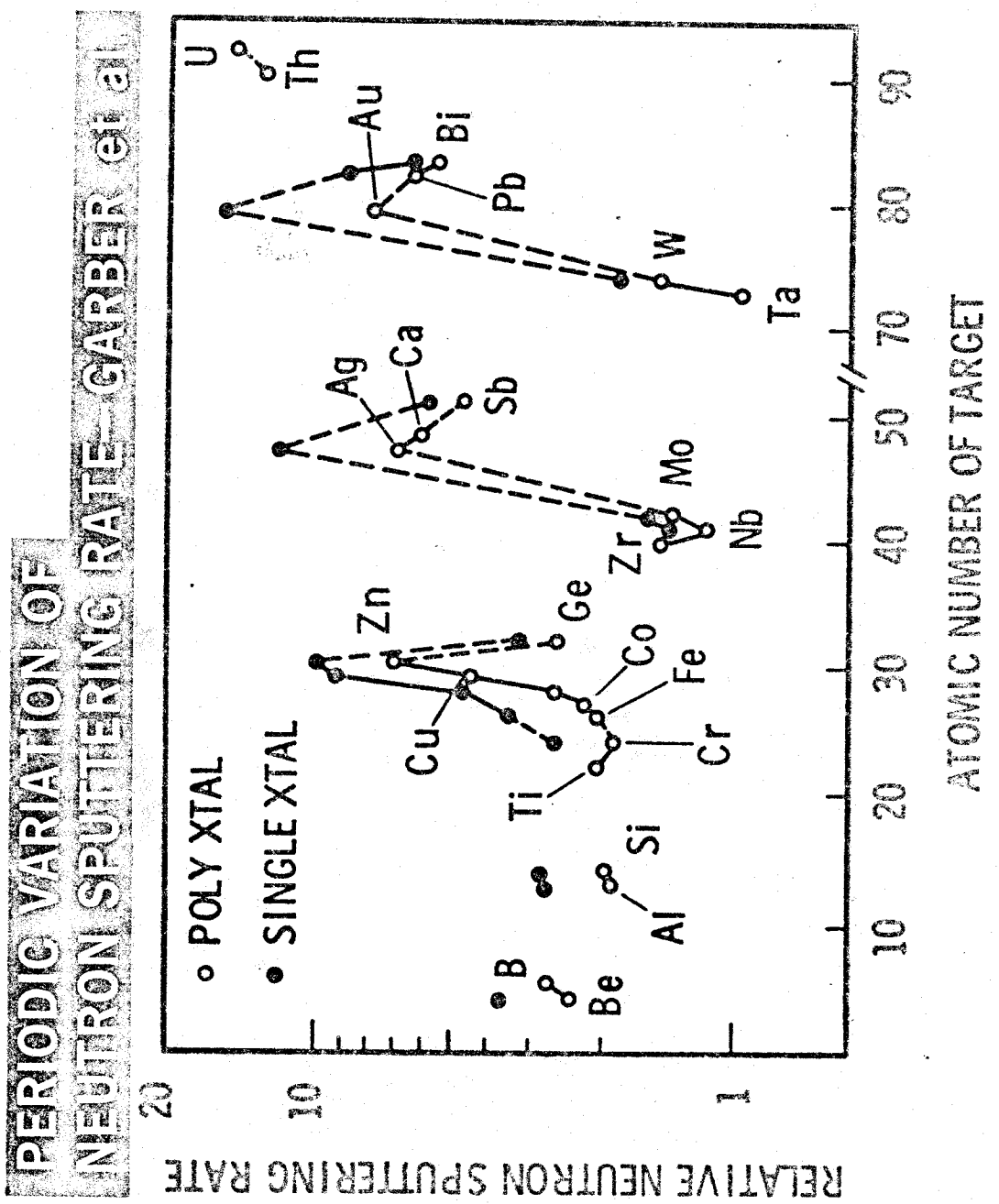

R. I. Garber, et. al., "Radiation Sputtering and Damage of Certain Metals in the Radiation Field of a Nuclear Reactor. Part 1. Sputtering by Fast Neutrons, " Atomnaya Energiya 28: 400, (May 1970).

PERIODIC VARIATION OF NEUTRON SPUTTERING RATE—GARBER et al.

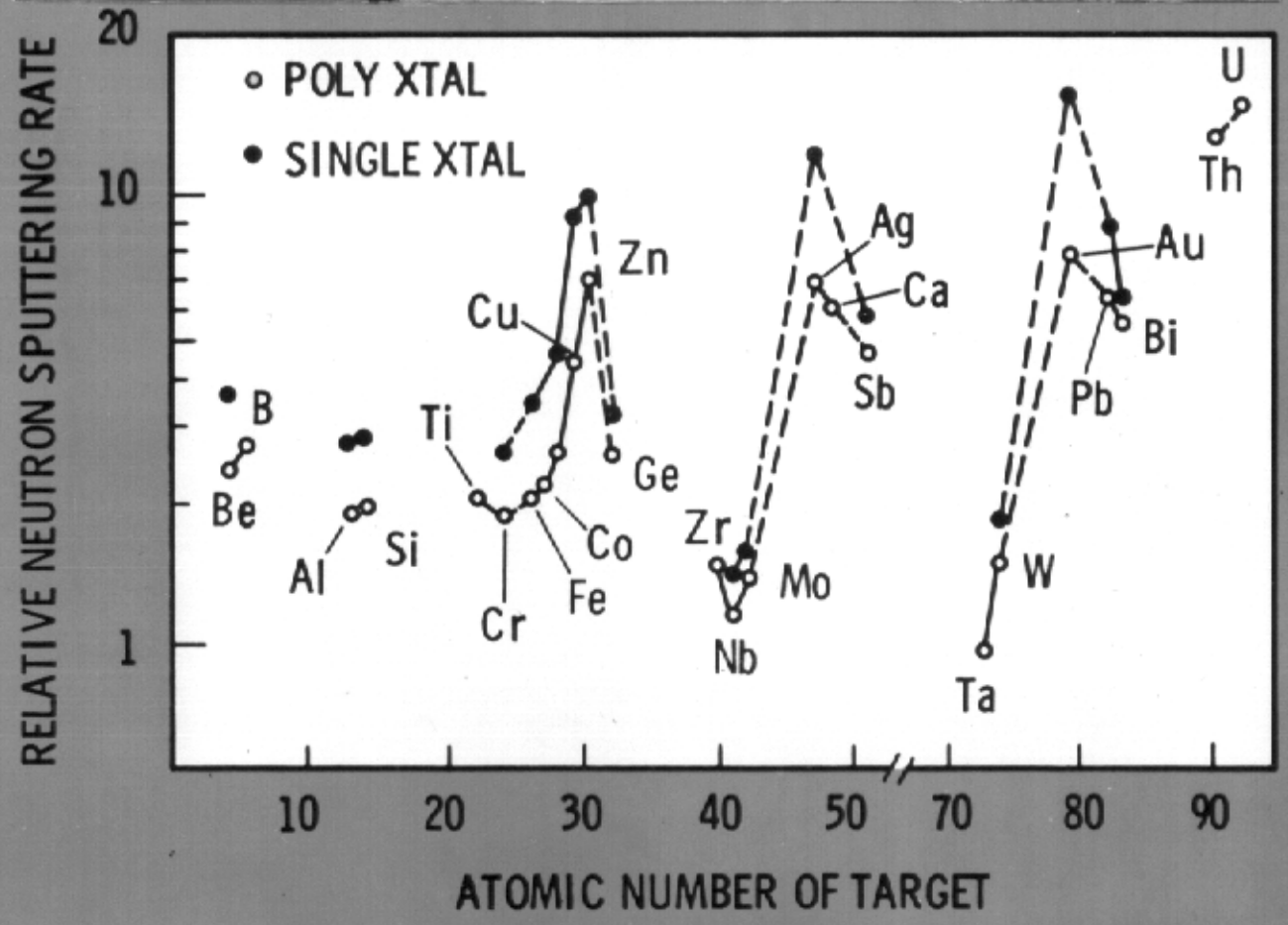

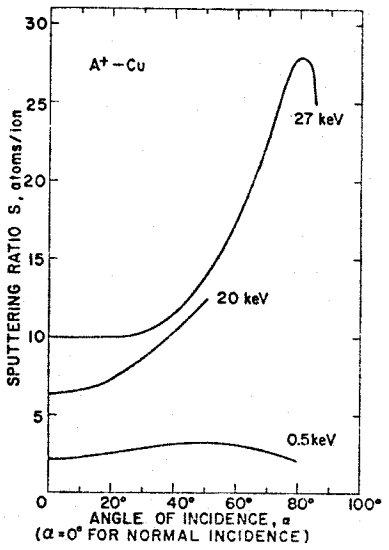

Variation of the sputtering ratio S with the angle of incidence α for argon ions incident on copper with energies of 27 keV (MOLCHANOV [*489*]), 20 keV (ROL et al. [*604*]), and 0.5 keV (WEHNER [*767*])

Figure 5

M. Kaminsky, Atomic and Ionic Impact Phenomena on Metal Surfaces, (Academic Press, New York), 1965.

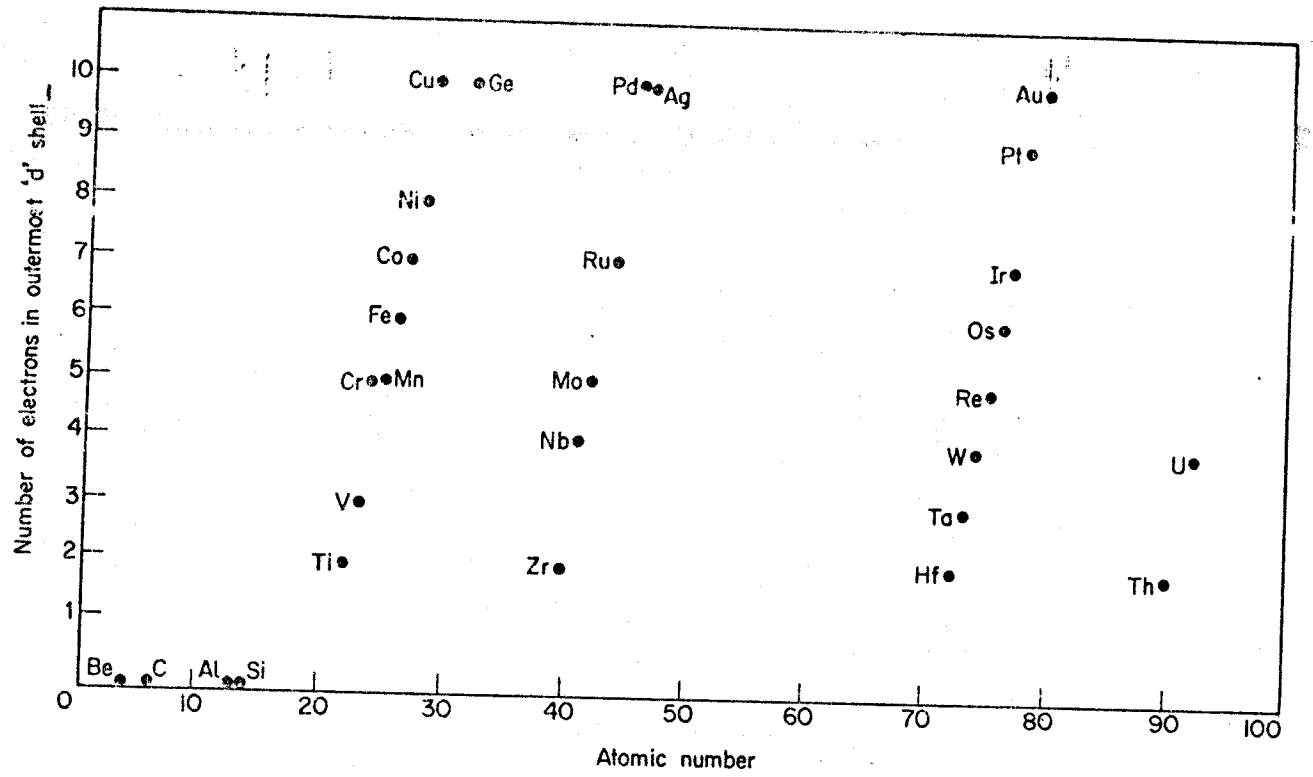

The number of electrons in the atomic 'd' shell as a function of the atomic number

Figure 6

G. Carter and J. Colligon, Ion Bombardment of Solids (American Elsevier Publishing Co., New York), 1968.

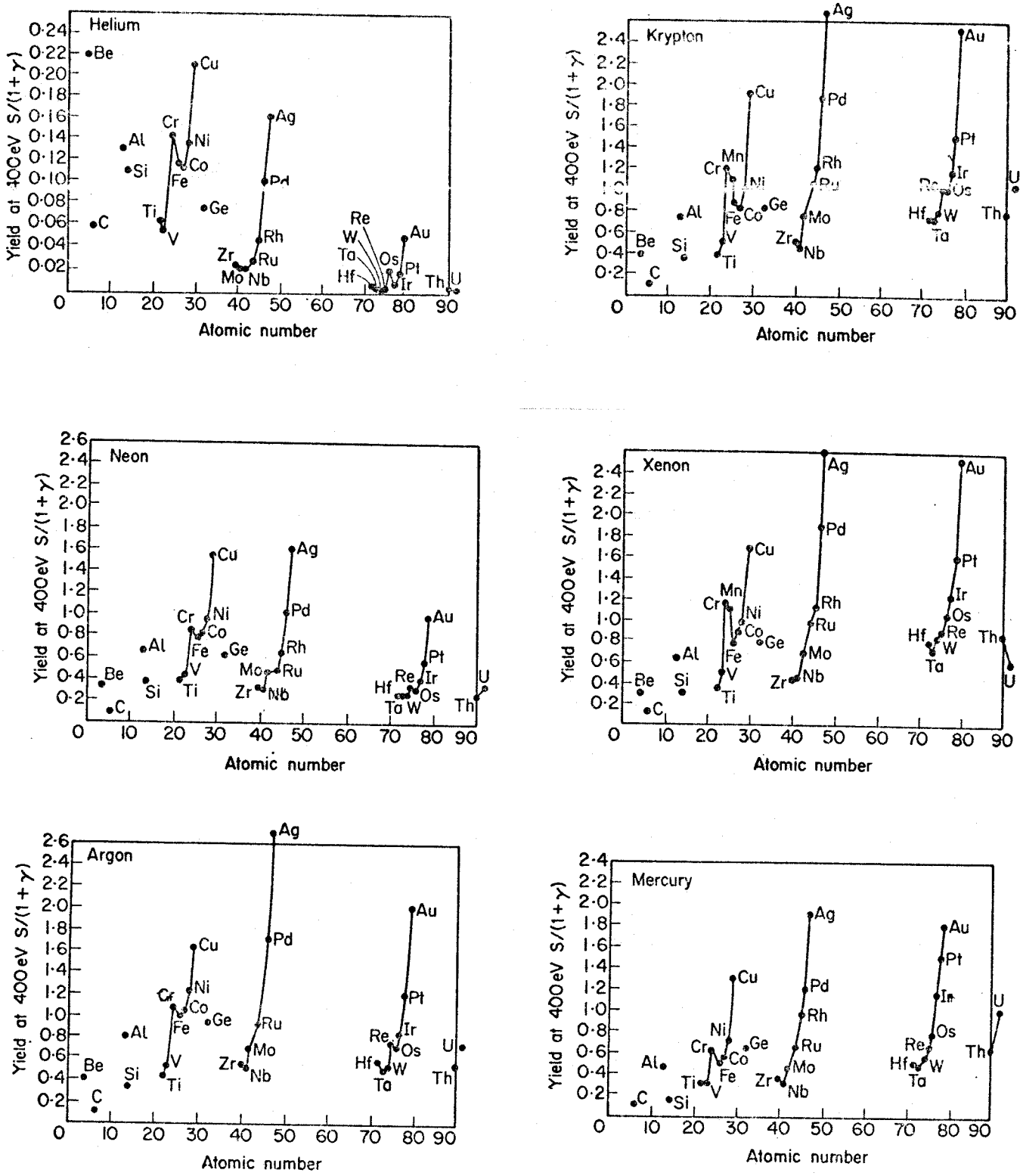

Variation of sputtering yield with atomic number of the bombardment material for 400 eV noble gas and mercury ion bombardment (viz. Refs. 7.36 and 7.37)

Figure 7

G. Carter and J. Colligon, Ion Bombardment of Solids, (American Elsevier Publishing Co., New York), 1968

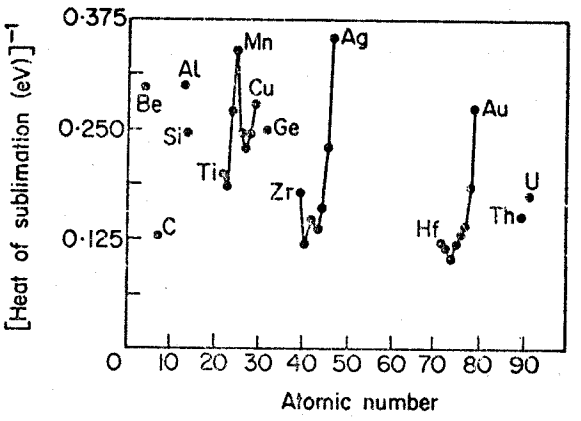

The reciprocal of the heat of sublimation as a function of atomic number

Figure 8

G. Carter and J. Colligon, Ion Bombardment of Solids (American Elsevier Publishing Co., New York), 1968.

HELIUM BLISTERING IN NIOBIUM

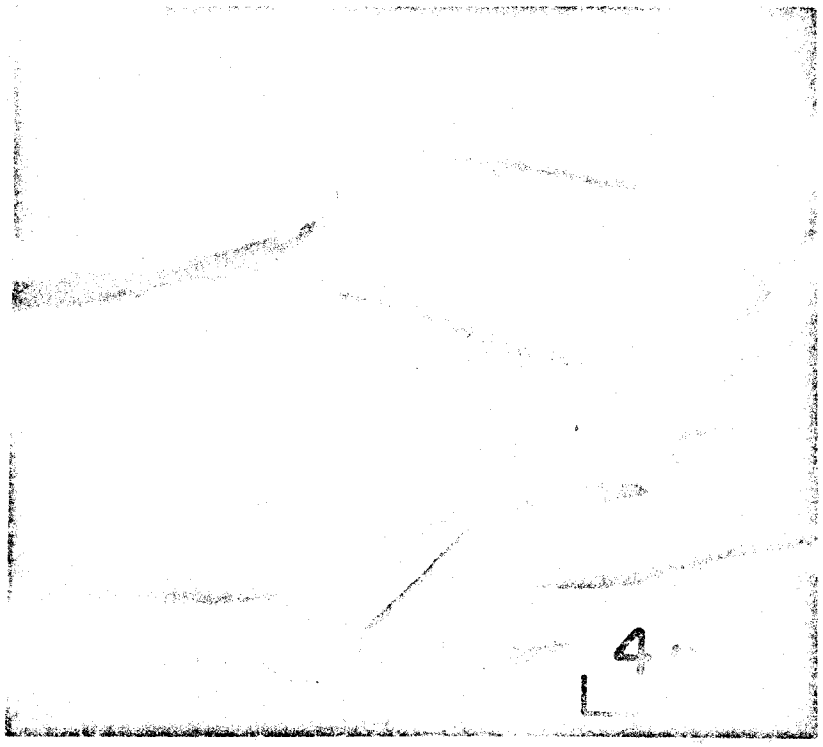

25°C

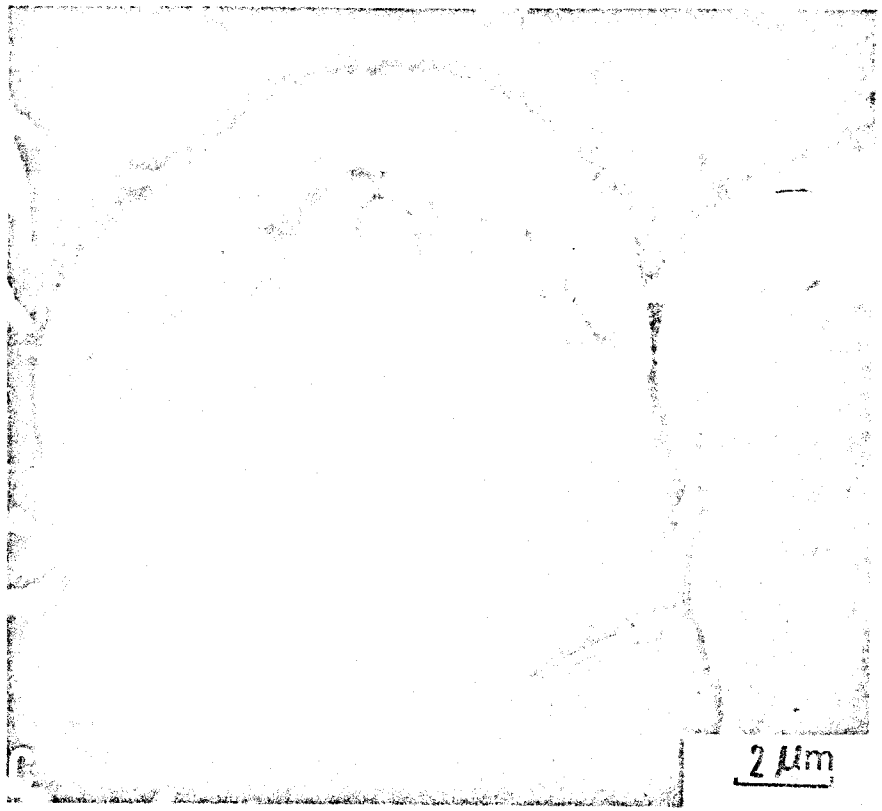

900°C

6×10^{18} He ions/cm^2 — 0.5 MeV

Figure 9

Figure 10

M. Kaminsky and S. K. Das, "Effect of Channeling and Irradiation Temperature on the Morphology of Blisters in Niobium," Appl. Phys. Lett. 21: 443, (Nov., 1972)

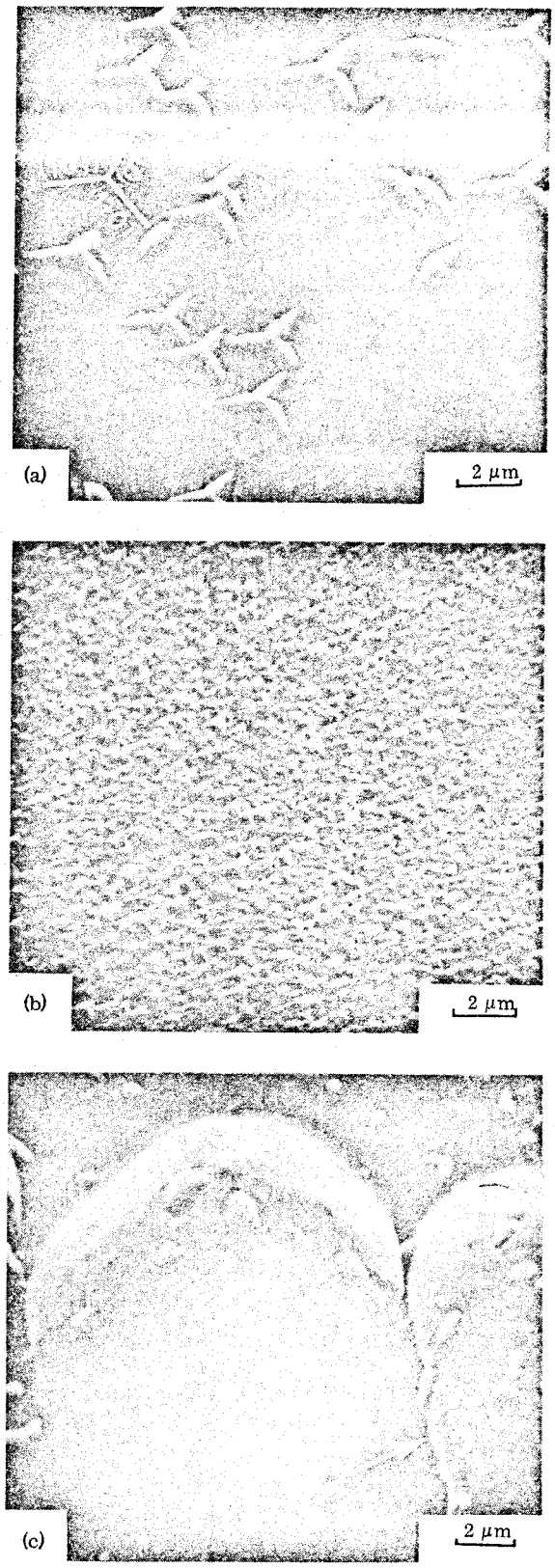

. Secondary-electron scanning electron micrographs of niobium surfaces after irradiation with 0.5-MeV He^+ at 900°C to a total dose of 1.0 C/cm^2 (a) in (111) Nb monocrystal for projectiles well channeled along the [111] axis, (b) in (111) Nb monocrystals for nonchanneled projectiles, and (c) in cold-worked polycrystalline Nb when the projectiles are incident normal to the target surface. All micrographs were taken with the specimen tilted 45° in the microscope, and a tilt correction was applied only in (c).

HELIUM BLISTERING IN NIOBIUM

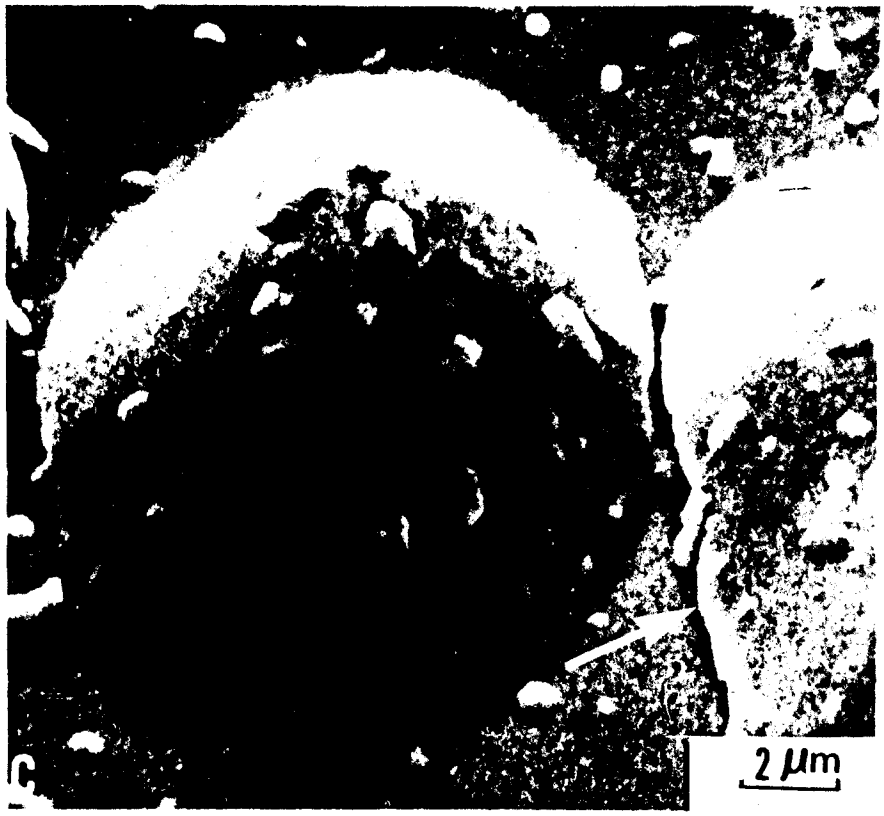

25°C

900°C

$6X10^{18}$ He ions/cm² — 0.5 MeV

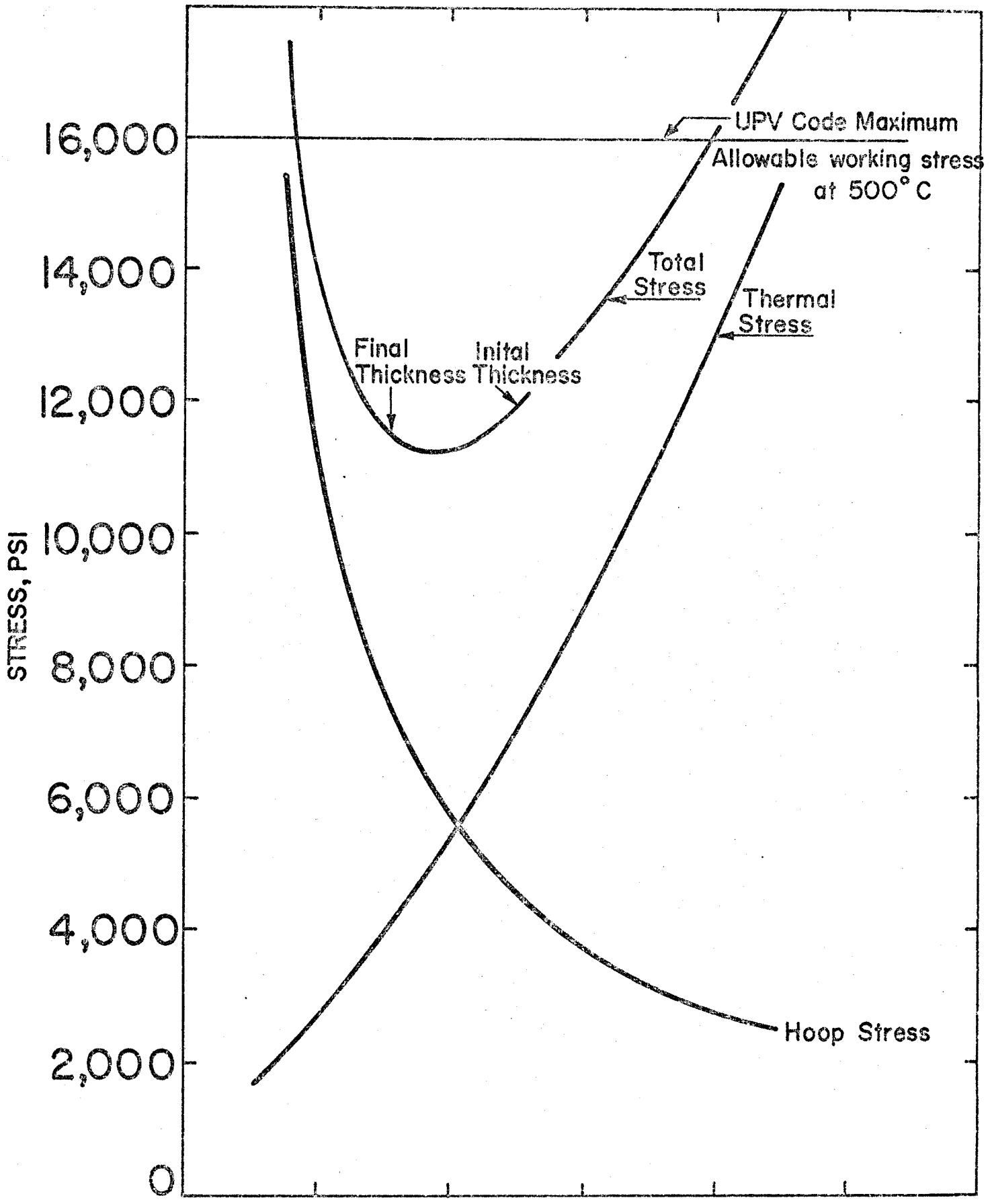

Figure 11 Stresses in the first wall as functions of wall thickness

FIGURE 12

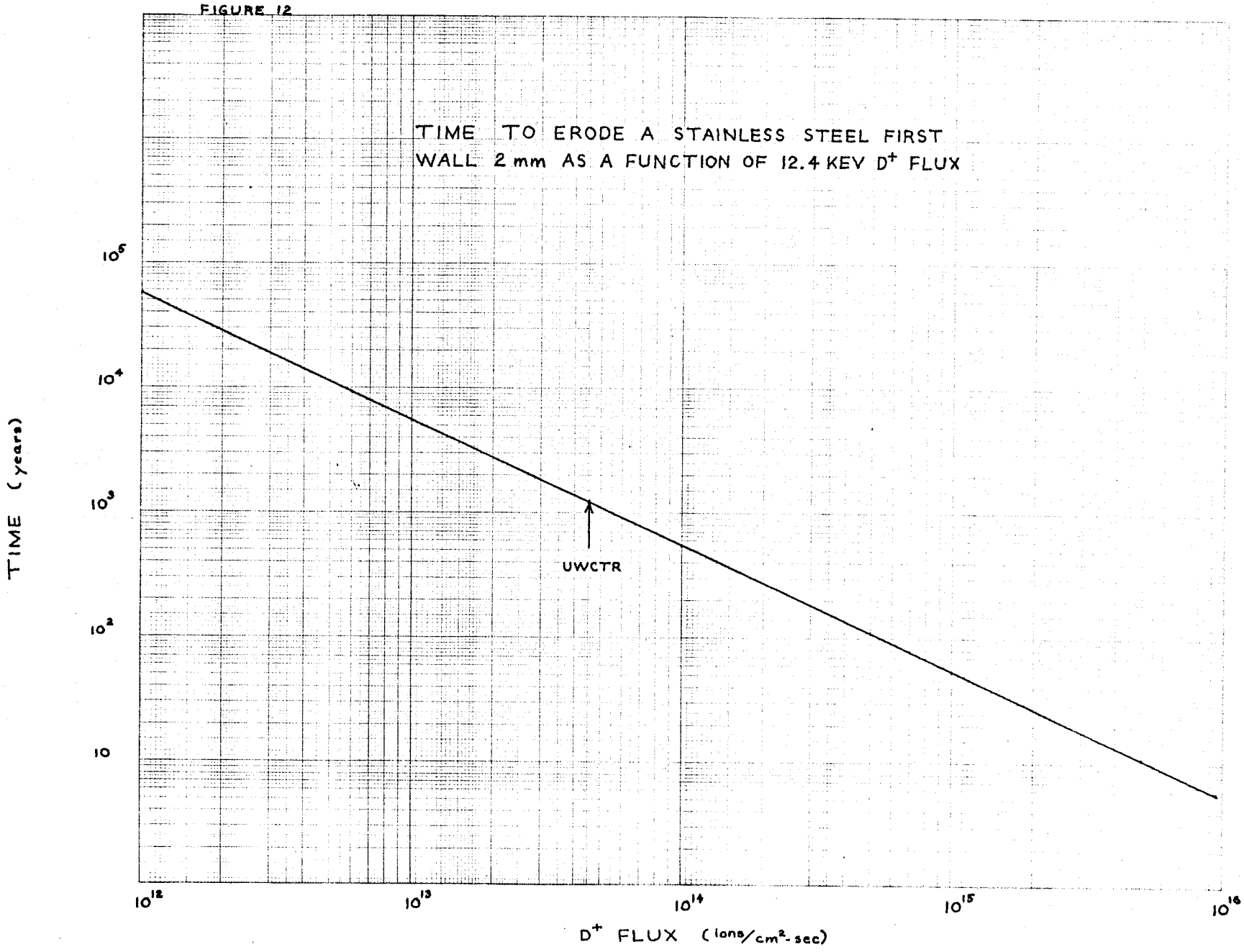

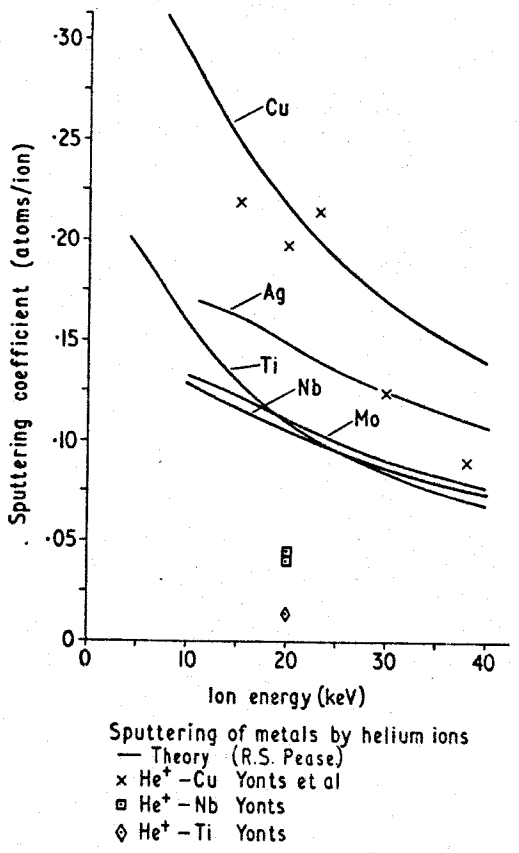

Sputtering coefficients for He^+ ions on various metals.

Figure 13

G. M. McCracken and S. K. Erents, "Ion Burial in the Divertor of a Fusion Reactor," Proceedings of the Nuclear Fusion Reactors Conference, BNES, Culham, p. 353, (September 1969).

Figure 14

TIME TO ERODE A STAINLESS STEEL FIRST WALL 2mm AS A FUNCTION OF 10 KEV ALPHA FLUX

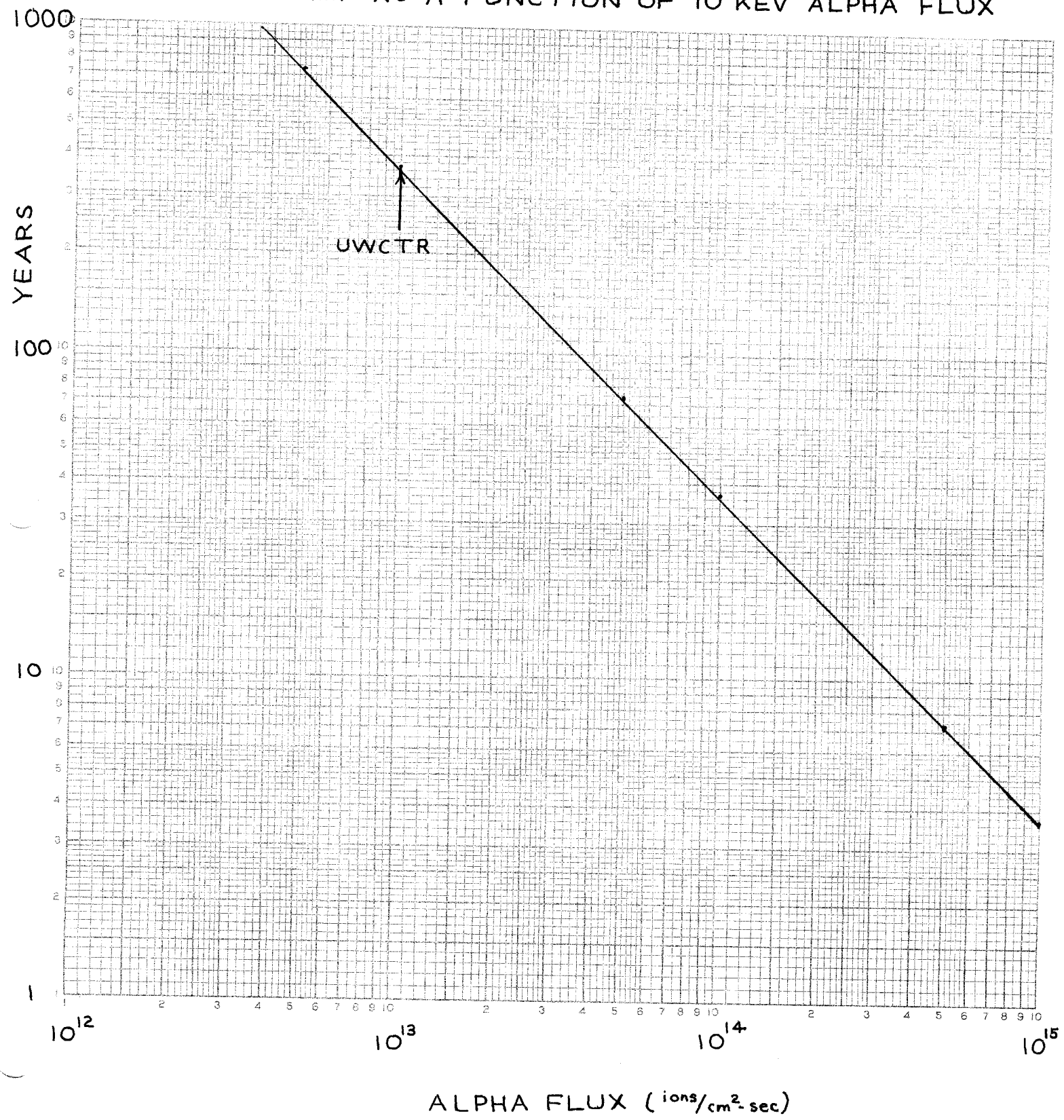

Full Logarithmic, 3 × 3 Cycles

FIGURE 15

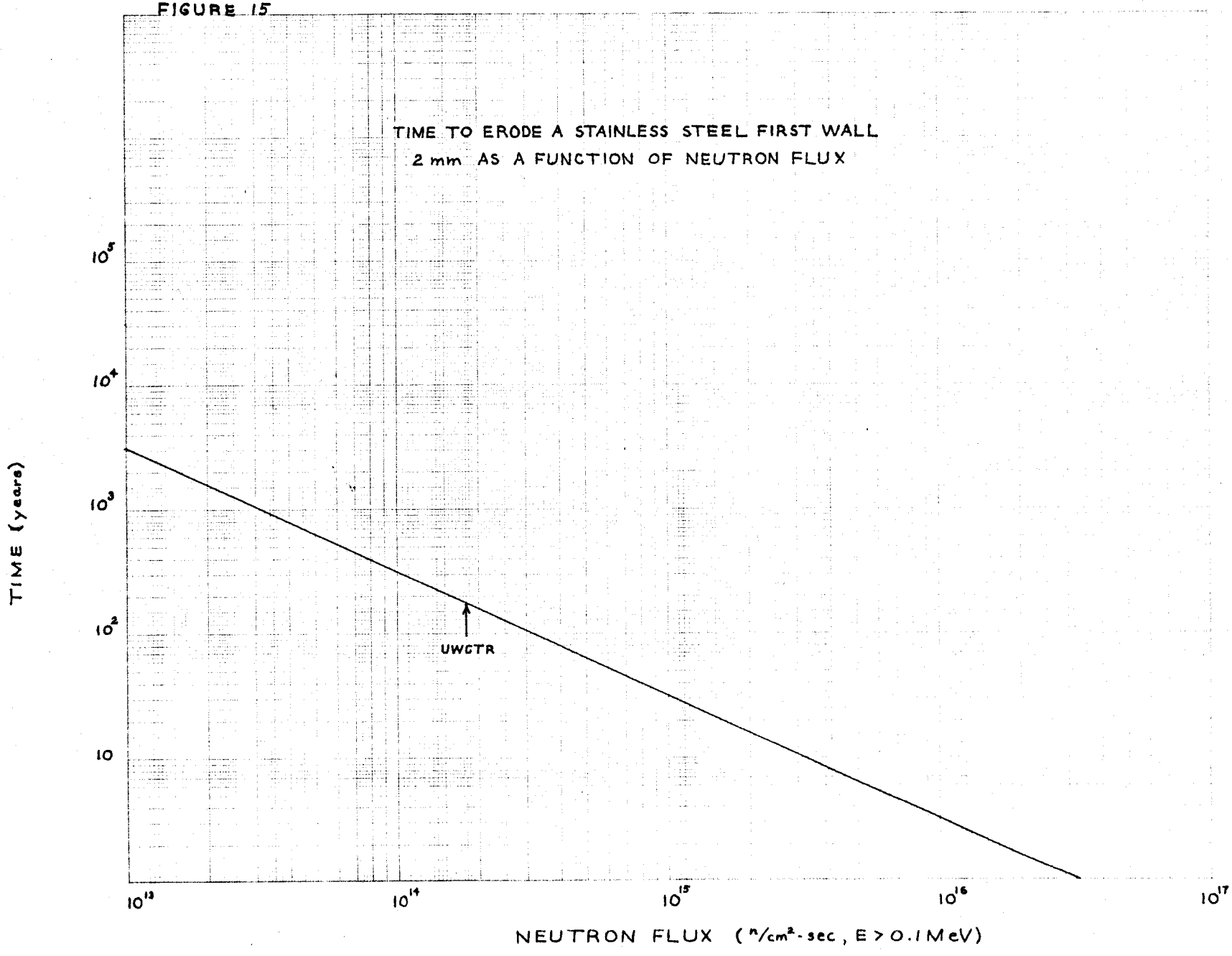
TIME TO ERODE A STAINLESS STEEL FIRST WALL
2 mm AS A FUNCTION OF NEUTRON FLUX
TIME (years)
10^5
10^4
10^3
10^2
10
UWCTR
10^{13}
10^{14}
10^{15}
10^{16}
10^{17}
NEUTRON FLUX (n/cm^2-sec, E > 0.1 MeV)

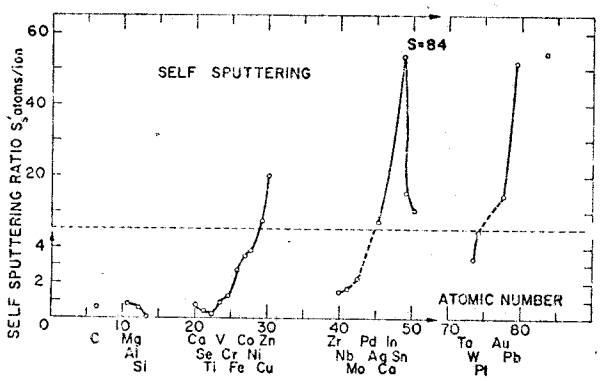

The self-sputtering ratio S_s for 45-keV ions as a function of the atomic number of the sputtering system ($Z_{target} = Z_{ion}$) (ALMEN et al. [*10*])

Figure 16

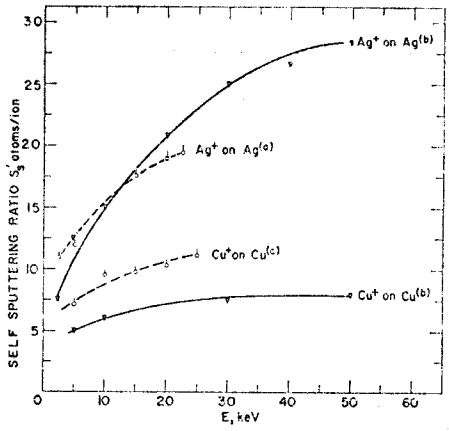

Variation of the self-sputtering ratio S_s with the energy E of the incident ion. Curves (*a*), GUSEVA [*274*]; curves (*b*), ALMEN et al. [*10*]

Figure 17

M. Kaminsky, Atomic and Ionic Impact Phenomena on Metal Surfaces, (Academic Press, New York), 1965.

Figure 18

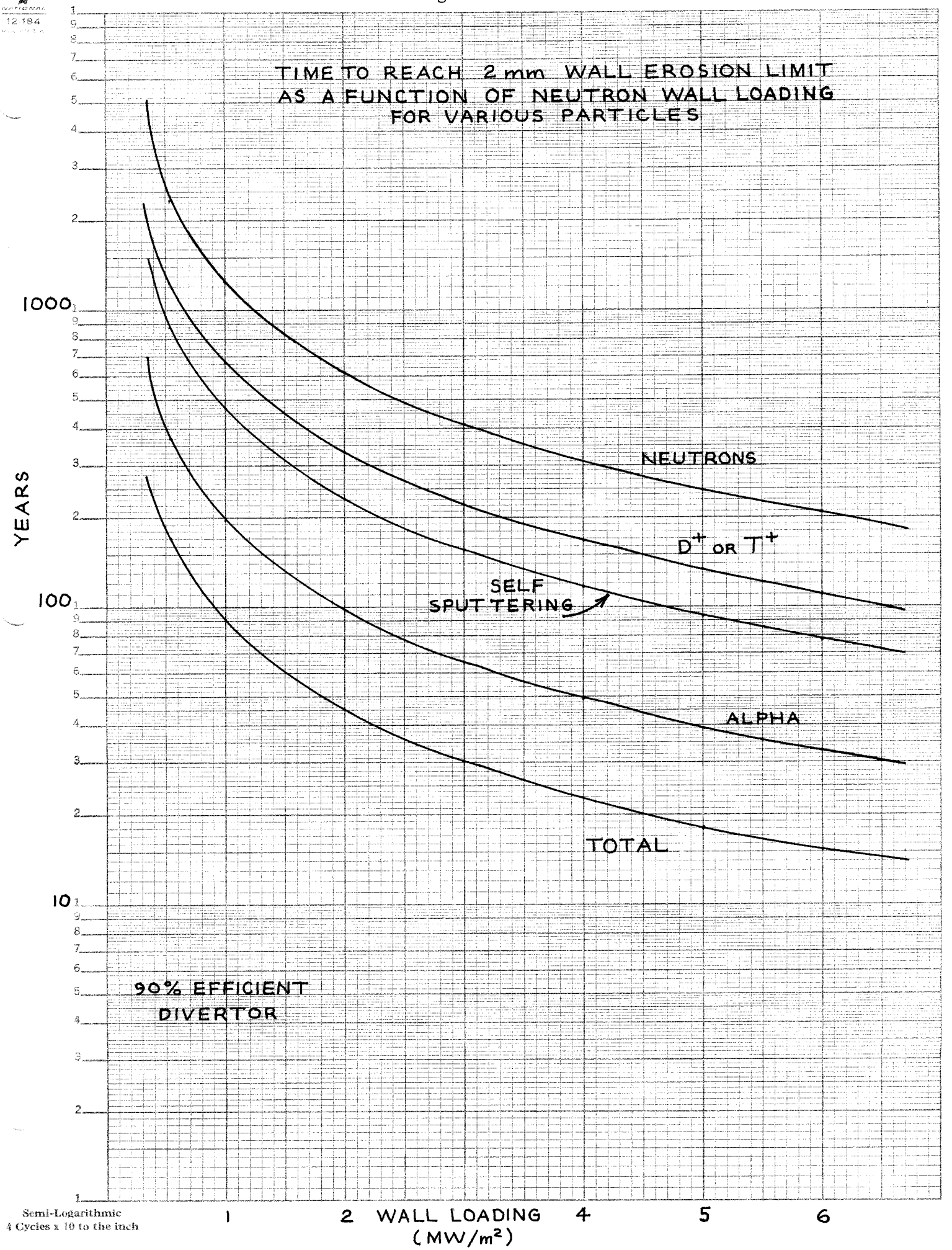

Semi-Logarithmic
4 Cycles x 10 to the inch

Figure 19

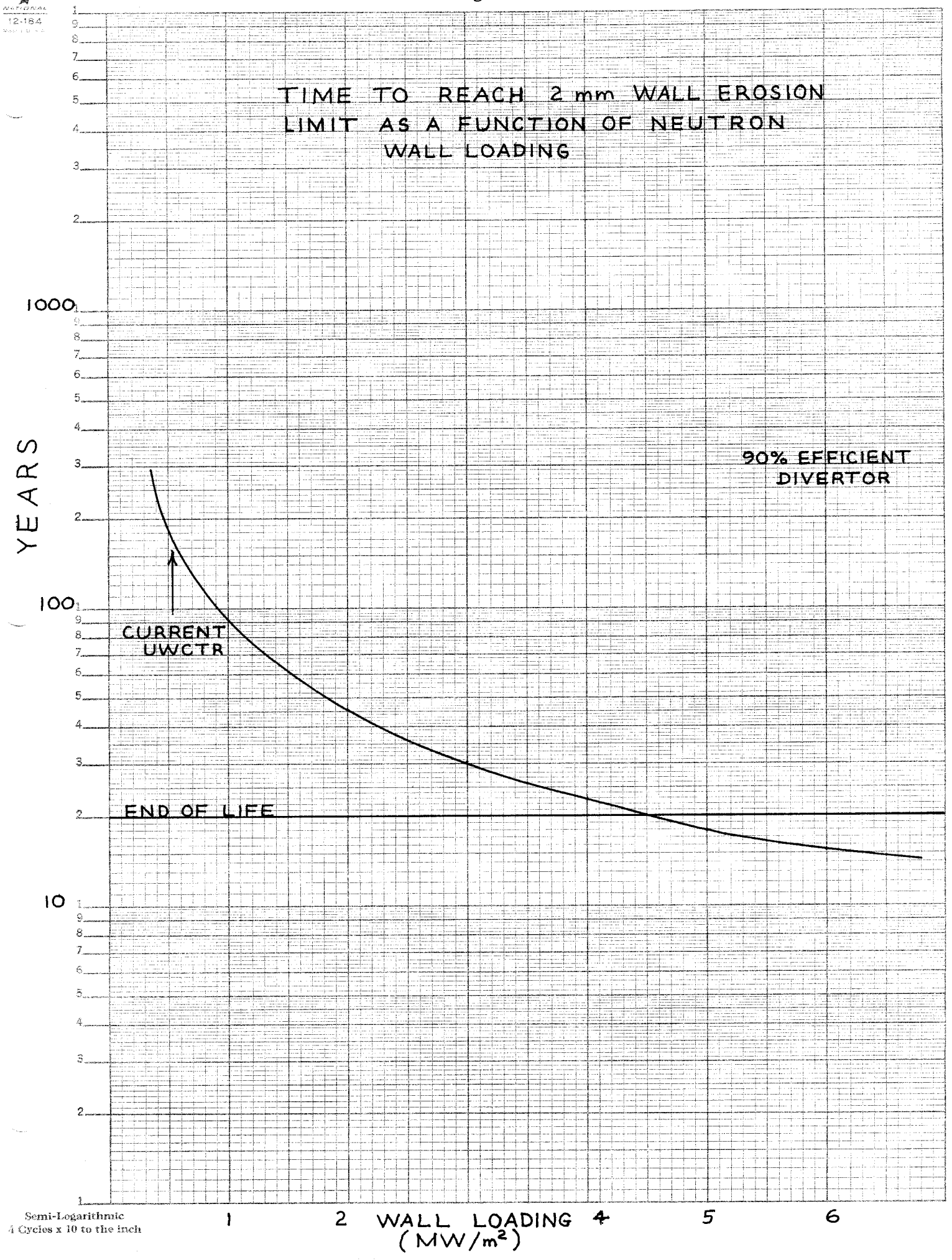

Semi-Logarithmic
4 Cycles x 10 to the inch